Operation and Maintenance of a High-Speed Water tunnel

by

Haynes Alexander M. Curtis

(Under the Direction of R. Benjamin Davis)

Abstract

The University of Georgia (UGA) High-Speed Water Tunnel (HSWT) has been in operation since July 2017. While existing literature provided much of the information needed to design the HSWT, literature covering the operation and maintenance of such a facility is sparse. To conduct experiments in a water tunnel requires unique tools and techniques that are not always intuitive. This thesis documents the development of foundational tools, equipment, and procedures necessary for the operation and maintenance of a high-speed water tunnel, and will serve as a reference and guide to those working with similar facilities. This thesis consists of four main sections including operational safety, experimental support devices, instrumentation, and maintenance.

Index words: Water Tunnel, Hydroelasticity, Modal Analysis

Operation and Maintenance of a High-Speed Water Tunnel

by

Haynes Curtis

B.S.M.E., University of Georgia, 2018

A Thesis Submitted to the Graduate Faculty
of The University of Georgia in Partial Fulfillment
of the
Requirements for the Degree

Masters of Science

Athens, Georgia

2018

Operation and Maintenance of a High-Speed Water Tunnel

by

Haynes Alexander M. Curtis

Approved:

Major Professor:	R. Benjamin Davis
Committee:	Donald Leo Brandon Rotavera

Electronic Version Approved:

Suzanne Barbour
Dean of the Graduate School
The University of Georgia
December 2018

Operation and Maintenance

of

a High-Speed Water tunnel

Haynes Alexander M. Curtis

December 2018

Acknowledgements

This work and education is dedicated to my family who have gone the extra mile to ensure that I have every resource needed to achieve my goals and pursue purposeful work.

A big thank you goes out to my close friends who continue to support me and place their trust in me. Thank you for everything, and I hope in some way I am able to return the favor.

My engineering education may well have not progressed to the graduate level if it were not for my bold and daring research advisor, Dr. Davis. He has truly led by example in that he always pushes outside of his comfort zone to solve increasingly difficult problems despite his many accomplishments.

I would also like to acknowledge the tremendous support provided by various teachers, professors, and mentors. From encouraging me to believe in my abilities, to pointing out my missteps, you have helped shape the person I am today.

Finally, a special thank you goes out to Lewis Fortner and the team of machinists at the University of Georgia UGA Instrument Shop. Without Mr. Fortner's contagious positive attitude, experience and extensive expertise, the construction of the water tunnel may not have been possible.

Contents

List of Figures

List of Tables

Chapter 1

Introduction

1.1 Overview

The University of Georgia (UGA) High-Speed Water Tunnel (HSWT) is a large variable-pressure closed-loop water tunnel that has been in operation at UGA since July 2017. The facility is designed and outfitted for hydrodynamic testing, emphasizing the study of fluid-structure interaction. The HSWT was designed and constructed in-house to achieve superior flow quality across a wide range of Reynolds numbers. The final design incorporates selective design elements from existing water tunnels such as the U.S. Navy's Large Cavitation Channel (LCC) and the High-Speed Cavitation Tunnel (HiCaT) at the University of New Hampshire [2, 3]. The test section measures 0.3 x 0.3 x 1 m^3 (12"x 12"x 39.4" in^3) with a maximum recorded flow speed of 12.2 m/s (40.0 ft/s). Turbulence intensities have been measured to be less than 0.5% above speeds of 1 m/s. After nearly two years of design and fabrication, the HSWT was installed in Driftmier Engineering Center. In the first year of operation, the facility yielded novel findings in the areas of underwater flutter, vortex-energy capture, and hydroelastic damping. In advance of renovations to Driftmier Engineering Center in Fall 2018, the HSWT was moved to Riverbend Research Laboratories.

Figure 1.1: The UGA high-speed water tunnel at Riverbend Research Laboratories, Fall 2018.

1.2 Scope

While existing publications provided much of the information necessary to design of the HSWT, information pertaining to operation and maintenance of such a facility is sparse. Water tunnels present a number of unique operational challenges, and solutions must be devised to effectively carry out experimentation. This thesis documents the development of foundational tools, equipment, and procedures necessary for the operation and maintenance of a high-speed water tunnel, and will serve as a reference and guide to those working with similar facilities. The content of this thesis culminates literature review, expert consultation, and firsthand experience carried out over four years. The four major sections include operational safety, experimental support devices, instrumentation, and maintenance. Operational safety refers to protocols developed to prevent structural damage to the tunnel and to protect the health and safety of operators. Experimental support devices refer to tools developed to

facilitate the collection of accurate and precise data within a water tunnel. Instrumentation encompasses the selection and design of devices that collect data. The maintenance section discusses the upkeep necessary throughout the service life of the tunnel.

1.3 Introductory Concepts and Terminology

This section introduces the concepts and terminology necessary to orient readers to water tunnel design and operation. Water tunnels come in a variety of shapes and sizes, each designed to meet a specific set of requirements. The central design goal of all water tunnels is to provide a controlled and repeatable environment in which to study the behavior of submerged structures in the presence of flowing fluid. The test section is the segment of the water tunnel where experimentation occurs (see Fig. 1.2), and objects created for testing are referred to as test articles (i.e. hydrofoils, scale models, etc.)

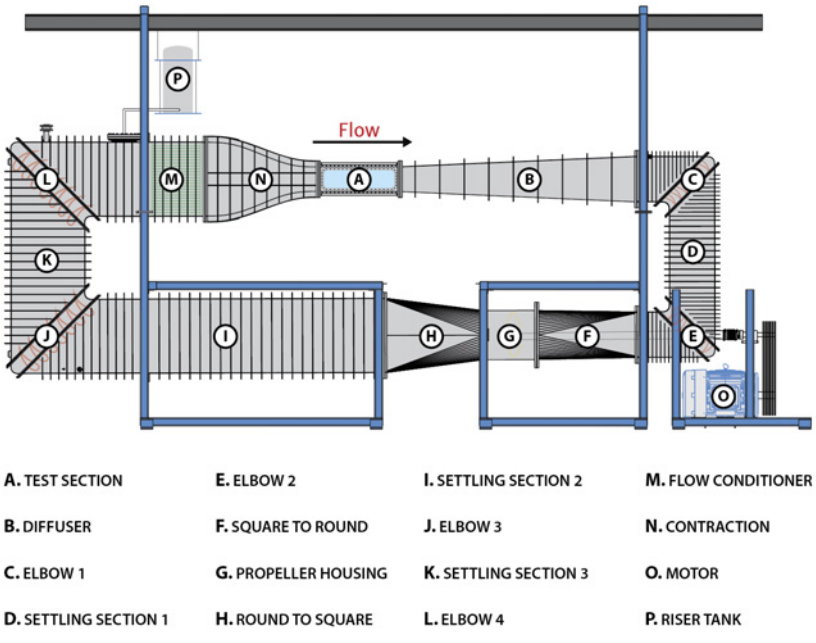

Figure 1.2: An annotated schematic of the HSWT.

Water tunnels are characterized and named by their testing velocity range, test section size, and their research focus. To provide a controlled and repeatable testing environment, the flow quality of the test section must be optimized. To achieve high flow quality, a low turbulence intensity and a uniform flow profile (see Fig. 1.3a) is desired throughout the volume of the test section [3]. Turbulence intensity, ψ, is defined in Equation 1.1 below:

$$\psi = \frac{u'}{U}, \tag{1.1}$$

where u' is the root-mean-square (RMS) of the instantaneous velocity minus the mean velocity at a fixed location over a given period of time, and where U is the mean velocity at the same location over the same period of time. A turbulence intensity between 1-3% is common for commercially manufactured water tunnels [4, 5], while specialized facilities such as the U.S. Navy's Large Cavitation Channel have achieved turbulence intensities below 0.1% with considerable effort and cost [3]. Turbulence reduction and flow uniformity is primarily achieved through use of flow conditioners including honeycomb matrices (Fig. 1.4a) and screens located upstream of the test section. However, flow conditioners are one of many factors affecting flow quality and measures are taken to reduce turbulence throughout the tunnel.

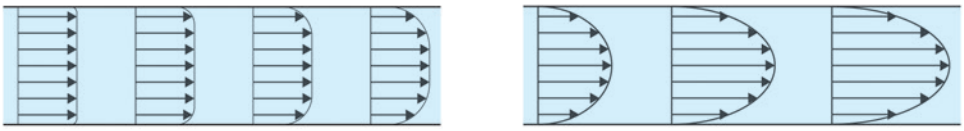

(a) (b)

Figure 1.3: (a) Development of a uniform flow profile with small deviations from centerline velocity (b) Development of a poor flow profile with large deviations from centerline velocity

Secondary means of turbulence reduction include the use of turning vanes to guide the water through each of the elbows (Fig. 1.4b) and high surface finishes within contraction

and diffuser sections. The contraction and diffuser sections of the HSWT are 304 stainless steel polished to a #8 mirror finish. Instrumentation and test article mounts within the test section must be designed and positioned to minimize flow disturbances. Various methods are used to visually map the flow quality in the test section, a process known as qualification, that is performed shortly after the tunnel is constructed or following major changes to the tunnel. A detailed description of water tunnel operating principles and qualification are discussed in [2, 3, 6].

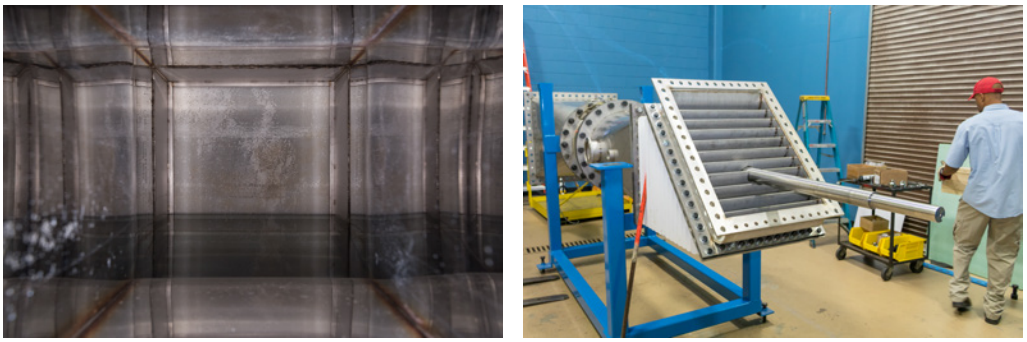

(a) (b)

Figure 1.4: (a) Plastic honeycomb matrix and contraction interior as seen from the entrance of the test section (b) One of four sets of turning vanes in the HSWT

1.4 Personal Contributions

A brief list of personal contributions involving the HSWT from Spring 2015 to Fall 2018 are provided below.

Undergraduate Contributions

- Literature review of existing tunnel designs and instrumentation
- Visitation to comparable facilities to consult experts on water tunnel design
- Flow-loop analysis to size pump and perform structural analysis

- Design of flow conditioner - sizing of the honeycomb, elimination of screens
- Assisted in initial qualification using Laser Doppler Anemometer
- Miscellaneous design recommendations including: viewport locations, bearing selection, shaft seal selection, and turning vanes

Graduate Contributions

- Designed and built a novel pneumatic hammer for modal testing within the test section
- Designed and installed the filtration and water management system
- Developed maintenance procedures for corrosion management and filtration
- Designed and assembled pressurized and gravity-fed dye injection systems for flow visualization
- Assisted in qualification using Laser Doppler Anemometer
- Modified force balance design from the University of New Hampshire
- Selected signal conditioner for use with the force balance and other strain-based measurements
- Selected and setup differential pressure sensor for mean flow velocity measurement
- Created educational media for the Dynamic Devices and Solutions Lab including posters, illustrations, images, and videos
- Assisted in lab relocation planning from Driftmier Engineering Center to Riverbend Research Laboratories
- Designed and installed pressure regulation system (riser tank)

- Assisted in experimental design for lab members and Gulfstream senior design teams
- Created water tunnel training videos for future generations of researchers performing experimentation in the HSWT

Chapter 2

Operational Safety

HSWTs are often large, costly, and potentially dangerous machines if operated improperly. Though one should always be mindful of hazards related to a specific experiment, this chapter will provide an overview of the most common dangers associated with normal water tunnel operation. These procedures pertain to averting structural damage to the HSWT and protecting the health and safety of operators.

2.1 Structural Hazards

The most likely cause of structural damage to the HSWT is improper pressurization. The HSWT was designed to withstand positive internal pressures and is susceptible to vacuum damage when the pressure inside the tunnel drops below atmospheric pressure. When draining or filling the tunnel, one or both of the vents must be in the open position to avoid structural damage.

To protect against overpressurization, a flange and stem are installed on the tunnel to accommodate interchangeable flange-mount pressure-relief discs. The relief discs should only serve as a secondary means of damage prevention. As a baseline reference, the tunnel should

not be operated above 6.9 kPa (3.5 psig) or below (0 kPa) 0 psig as read by the pressure gauge connected to the riser tank (Sec. 3.2). This reference is subject to change over time due to modifications to the tunnel, and only reflects the suggested pressure limits at the time of publication.

Figure 2.1: The flange and stem assembly added to accept flange-mount pressure-relief discs.

2.2 Powerplant Hazards

The drive system of the HSWT is an entanglement hazard, similar to other large rotating machinery such as a mill or a lathe. Safety gates have been installed around the motor to prevent accidental contact with the belt and pulley system. The gates should only be removed during service of the belts, bearings, or motor. In any case where the safety gates are removed, as shown in Figure 2.2, the power supply for the motor should be locked out.

Should the tunnel be drained completely, the motor should never be run while the tunnel is dry. The cutless bearing (Fig. 2.2b) that supports the drive shaft near the propeller uses water as a lubricant during operation. Running the motor while the bearing is dry, even for a brief moment, will destroy the bearing.

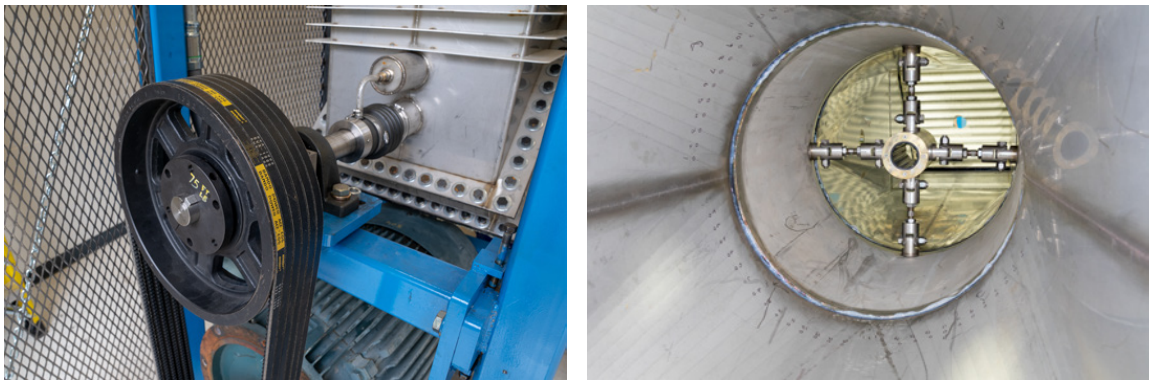

(a) (b)

Figure 2.2: (a) The drive system of the HSWT as seen with a safety gate removed. (b) The internal cutless bearing used to support the propeller drive shaft.

2.3 Noise

Per the U.S. Occupational Safety and Health Administration (OSHA) recommendations for general industry worksites [7], the current Permissible Exposure Limits (PELs) are listed in Table 2.1 below:

Duration	**PEL**
8 hours	90 dBa
4 hours	95 dBa
2 hours	110 dBa
1 hours	105 dBa
30 minutes	110 dBa
15 minutes	115 dBa

Table 2.1: A summary chart of OSHA's maximum recommended exposure durations, specified in 5 Decibel (dBa) increments.

The HSWT's motor produces between 85-95 dBa during normal operation. Therefore, it is highly recommended that hearing protection be worn, especially during prolonged periods of operation.

2.4 Electrical

The tap water used to fill the water tunnel contains natural minerals, metals and other ions that make it an electrolyte. As such, tunnel operators using electronic equipment near or in the tunnel should take precautions to protect themselves from harmful or fatal electrical shock. When the top of the test section is removed, electronic devices and power strips should be positioned away from the test section to reduce the risk of electrical contact with water. Devices such as ground-fault interrupters can be used as a protective measure against electrical shock.

Figure 2.3: Front panel of variable frequency drive

The variable frequency drive (VFD) used to control the motor contains a design flaw that is a potential explosion hazard (Fig. 2.3). A very small gap is placed between the front plate and high voltage contacts such that enough pressure on the front plate could cause contact across the voltage sources. A small piece of fiberglass has been installed to reduce the risk of contact. Avoid leaning or pressing on the outer casing of the VFD, especially while the tunnel is operating. The piece of fiberglass should not be removed under any circumstances, nor should the VFD or any of the electrical boxes be opened while the tunnel is in operation.

Chapter 3

Experimental Support Devices

Experimentation in a water tunnel requires the use of specialized equipment designed to withstand the operating conditions of the test section. Experimental support devices are tools that facilitate the collection of accurate and precise data within a water tunnel. This section details a series of basic tools and techniques devised for the HSWT. Methods used to secure test articles and insert instrumentation into the flow are discussed before introducing devices designed to meet specific needs. These specialized devices include a pressure regulation system, pneumatic hammer for modal testing, traverse system, and safety bracket.

3.1 Windows

The test section windows of a water tunnel are used for observing test articles, and serve as the primary surface to which test articles are secured and instrumentation is inserted into the flow. Introducing test articles and instrumentation into a water tunnel presents a number of challenges, including the need for water-tight seals and the need to minimize flow disturbances in the test section.

Window design begins with choosing the correct material to handle the loads involved with specific applications. Windows for water tunnels are commonly made of acrylic, metal, or glass. This section covers each type of window material and application examples in the HSWT. Table 3.1 provides a summary of each material type and properties relevant to water tunnel applications.

Material	**Cost**	ρ $[g/cm^3]$	σ_{yield} **[MPa]**	**Expansion Coeff.** $[\mu m/^\circ C]$
Cast Acrylic	Medium	1.19	70	77.0
Aluminum (6061-T6)	Low	2.70	270	23.6
Plate Glass	High	2.51	33	3.25

Table 3.1: A summary chart of common window materials and relevant properties for water tunnel operation [1, 2].

3.1.1 Acrylic Windows

Water tunnel windows are most often constructed from acrylic due to its affordability, machinability, and durability. Though optically inferior to plate glass, acrylic provides acceptable optical clarity for many types of laser-based instrumentation systems and for qualitative experiments involving flow visualization. The primary drawback of acrylic is that it is easily scratched, chipped and cracked (see Fig. 3.1).

Figure 3.1: Scratches on the bottom acrylic window of the test section.

While scratch resistant acrylics are available, their cost is higher than unprotected acrylic. Accumulation of scratches may render a window optically useable over time. In some cases, the surface of the acrylic can be sanded and polished to renew the surface. The coefficient of thermal expansion for acrylic is high as compared to metal and plate glass, which can make the windows challenging to install when warmed through seasonal temperature changes or operation.

The acrylic windows designed for the HSWT are constructed from 50.8 mm (2") thick cast acrylic sheets (Fig. 3.2). While more expensive, cast acrylic provides more homogenous material properties over extruded acrylic that are desirable for optical clarity, machinability, and resistance to pressure. The HSWT test section frame is dimensionally identical on all sides, allowing windows to be interchanged. A 3.175 mm (1/8") thick stainless steel retaining ring is used with acrylic windows to distribute the pressure of the cap screws evenly around the perimeter of the window. The distribution of pressure not only promotes even pressure for sealing, it also prevents the acrylic windows from cracking under the load of the cap screws.

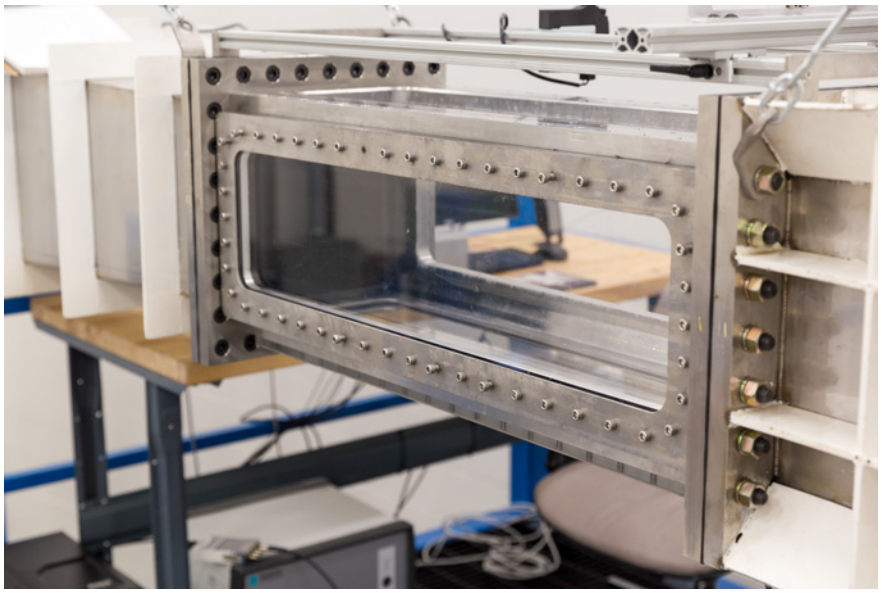

Figure 3.2: The front of the test section with an acrylic window and retaining ring.

Modifying acrylic windows to accommodate test articles and instrumentation should be done with caution. Removing large portions of the material may induce undesirable stress concentrations, causing the window to break during handling or testing. An acrylic window modified for use with the force balance (Sec. 4.2) cracked within the first several weeks of use, and was subsequently replaced with an aluminum window (Sec. 3.1.2). Acrylic window modifications for the HSWT include the installation of a pressure tap on one window and a pattern of threaded holes on another window. A 1/8" NPT to 1/4" push-to-connect tube fitting is installed near the end of an acrylic window along the centerline to allow pressure measurements to be taken in the test section (Fig. 3.3a). A counterbore is drilled into the acrylic such that the fitting is flush to the inside of the window to minimize flow disturbance in the test section. A plastic fitting is used to prevent the acrylic from cracking during installation.

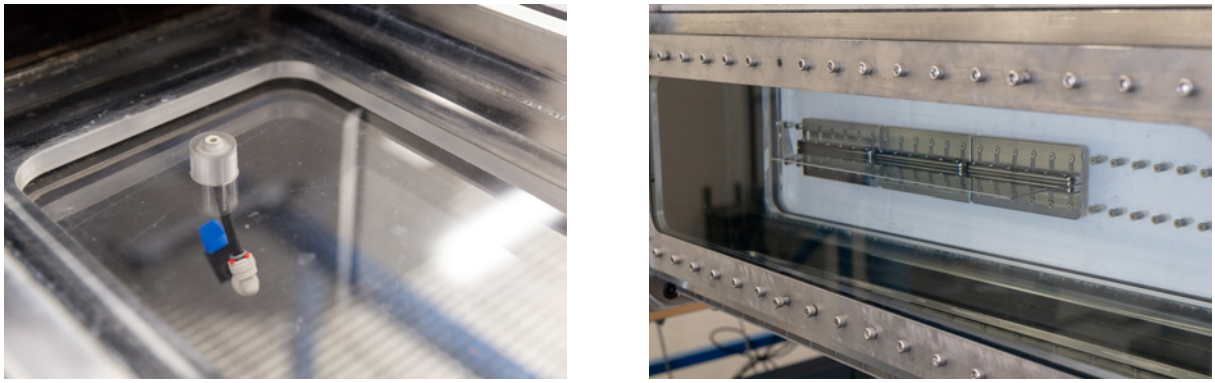

(a) (b)

Figure 3.3: (a) A pressure tap installed on an acrylic window with push-to-connect tubing attached. (b) The 'breadboard' acrylic window with a flat plate secured inside the test section. A piece of foamcore has been place in the background to improve visibility.

A series of evenly spaced 1/4"-20 threaded holes are installed on a second acrylic window, permitting test articles to be directly mounted to the window (Fig: 3.3b). This 'breadboard' hole configuration is useful for long test articles, such as flat plates, that must be clamped down the length of the test section. Each hole is outfitted with a metal insert to protect the

acrylic threads from being worn down by the metallic screws. To minimize flow disturbances, unused holes are plugged with flat-head countersink screws.

3.1.2 Metal Windows

Metal windows are used when acrylic windows may develop undesirable stress concentrations and become prone to cracking. While many metals offer superior strength as compared to acrylic, the disadvantages include galvanic corrosion (Sec. 5.2), weight, and optical opacity. Aluminum is a metal commonly chosen for the construction of specialty water tunnel windows because of its affordability, strength, ease of machining, and ability to be anodized. Though stainless steel will not corrode in a water tunnel constructed of the same type of stainless steel, the cost of constructing a stainless steel window often far exceeds the cost of adding a protective coating to a less expensive metal.

At the time of publication, two aluminum windows are used with the HSWT including a top plate with a grid of 3/4"-16 threaded holes and a window used to insert the force balance (Sec. 4.2). The aluminum top plate (Fig. 3.4a) is primarily designed to accept cable glands, more commonly referred to as cord grips.

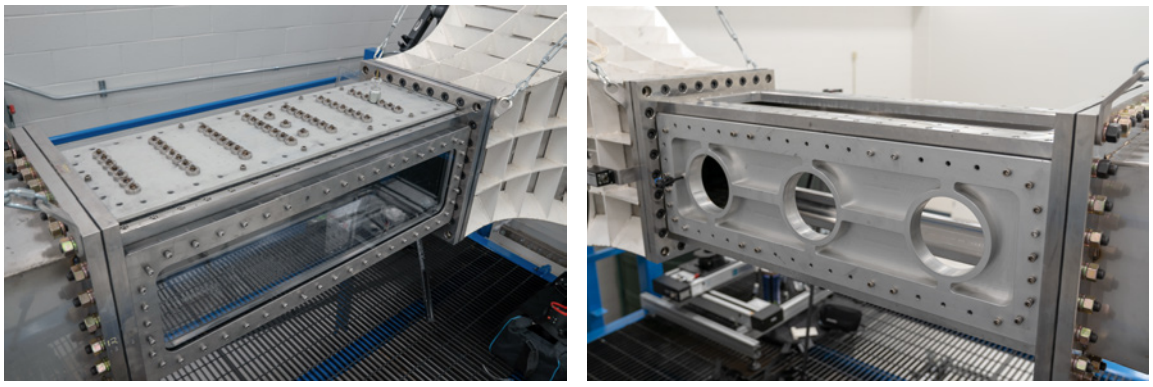

(a) (b)

Figure 3.4: (a) The aluminum top plate used for chord grip insertion. (b) The bare force balance window without the force balance or solid plugs installed.

Cord grips are traditionally used to pass a cord or cable into an electronics enclosure (Fig. 3.5a). They seal electrical connections from outside contaminates such as dirt, oil, and moisture and provide strain relief for the cables being fed into the enclosure. Cord grips are readily available through commercial hardware suppliers in a variety of shapes and sizes. The internal rubber gland (Fig. 3.5b) that is compressed to form a seal can be interchanged to accommodate the diameter of the cord or object being passed through it. For high-speed water tunnels, cord grips serve as an indispensable means to insert various devices into the test section while maintaining a secure water-tight seal. For example, chord grips have been used to insert dye injection nozzles (Figure 3.5c) into the flow (Sec. 4.3).

(a) (b) (c)

Figure 3.5: (a) A chord grip as seen on an electronics enclosure. (b) A disassembled chord grip. (c) A chord grip installed on the aluminum top plate to facilitate dye injection in a closed channel.

Chord grips can be used to feed data or power cables into and out of the test section. Many chord grips are commonly equipped with tapered threads and may require an adapter to attach to the test section. Due to the depth of the holes on the top plate, straight 3/4"-16 straight threads were selected for ease of machining and an adapter is used to convert from the tapered thread on the cord grip to the straight internal threads of the top plate. Teflon tape is used on the threads to promote a water-tight connection.

The top plate was originally intended as probe insertion points for a constant temperature anemometer (CTA) and while the design is functional, the top plate design requires improvements. The excess material should be milled out from the top to reduce weight for ease of handling. Removing material from the top would also allow for more efficient movement of the CTA probe from one location to another. The threaded holes are too deep to allow the 90 degree probe support to be maneuvered into the test section, requiring the window to be completely removed change probe locations. Each of the plugs fabricated for the top plate are custom machined, adding unnecessary cost to the construction of the aluminum top plate. During initial design, the hole size, location, and spacing could have been modified such that standard bolts could be used as plugs with little to no modification required. The top plate was not anodized initially and quickly began to corrode. The rough surfaces created by corrosion before the window was anodized negatively affected the effectiveness of the anodization. As a result, corrosion takes place in localized areas.

The second aluminum window (Fig. 3.4b) is designed to mate with the force balance discussed in Section 4.2. Having learned from the construction of the aluminum top plate, 9 kg (20 lbm) of excess material were removed and the window was anodized immediately after fabrication. A clear anodization coating is applied to both aluminum windows, making it challenging to monitor the condition of the coating. A colored coating would have been preferred to visually monitor the condition of the coating.

3.1.3 Glass Windows

Plate glass is optically superior to acrylic and can be used for the construction of water tunnel windows. Low iron glass provides high optical clarity and is commonly used in high-end aquariums. While the optical clarity of plate glass surpasses that of acrylic, plate glass is exceptionally difficult to machine, expensive, heavy, and brittle. Glass windows are used for specialty applications [2] and to date a glass window has not been necessary for the HSWT.

3.2 Pressure Regulation System

Pressure regulation of a water tunnel allows the operator to protect the tunnel's structure, eliminate unwanted air from the flow loop, and control cavitation. Due to the large pressure reduction across the contraction, sections of the tunnel between the contraction and pump inlet are regularly below atmospheric pressure. Low pressure conditions can cause unwanted structural loading, air bubbles, and cavitation within the tunnel. A common solution to address these issues is referred to as a riser tank (see Fig. 3.6) — an expansion reservoir placed above the water line of the tunnel.

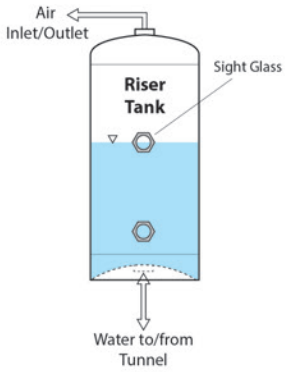

Figure 3.6: Illustration of a riser tank

During normal operation, a water tunnel expands and contracts due to fluid forces and thermal expansion effects. As the tunnel expands and contracts, the free surface in the riser tank will rise and fall to account for changes in the tunnel's volume. This enforces a consistent pressure throughout operation, promoting controlled experimentation and preventing structural damage. For tunnels designed to withstand pressures above or below atmospheric pressure, a riser tank can also be connected an air compressor or vacuum pump to control the static pressure of the water tunnel.

3.2.1 Design Goals

For the first year of operation, the HSWT was filled and vented manually to assess the need for a riser tank. Manual regulation presented a number of challenges that ultimately justified the cost of installing a riser tank. These challenges include experimental consistency, operator safety, and structural safety of the tunnel. During operation, the tunnel was manually filled and vented to regulate pressure, which is interruptive to the operator's work flow and caused variations in tunnel pressure throughout an experiment. The interruptive nature and safety risks of manual regulation were amplified by the vent locations, which were only accessible by ladders. With no way to monitor the water level in the tunnel from the location of inlet shutoff valve, filling the tunnel resulted in water spouting from the vents onto the lab floor before the operator could reach the shutoff valve. With these experiences in mind, a list of design requirements was formulated for the riser tank system as outlined in Table 3.2.

Design Goal	**Description**
Additional Water Volume	Sufficient water volume must be present to account for tunnel expansion, contraction and pressurization
Factor of Safety	Components must not impose reduced operating limits on the tunnel
Compressed Air Connection	Connection to an air compressor via quick connect
Corrosion Resistant	Components must be resistant to corrosion in the presence of 304 stainless steel
Accessibility	Operational valves must be easily accessible on the tunnel mezzanine
Water Level Indicator	Water level in the tank must be visible from the mezzanine or lab floor
Self-Regulation	Riser tank should require little to no attention from the operator
Redundancy	Must prevent the formation of undesirable structural loads

Table 3.2: Riser tank design requirements

3.2.2 Design Process

The riser tank volume was estimated by deliberately overfilling the tunnel to its maximum design pressure of 127 kPa (1.25 atm) and measuring the water removed to bring the tunnel back to atmospheric pressure. This method revealed that a minimum of 18.9 L (5 gal) would be required to account for pressure expansion alone. A commercially manufactured 30 gallon retention tank (Amtrol, ERTG-30) was chosen to provide ample water volume for expansion due to pressure, thermal effects, and operational fluid forces (Fig. 3.7a). Beam clamps, threaded rods, and steel plates are used to suspend the tank from the beam above the HSWT.

(a) (b)

Figure 3.7: (a) Riser tank installed over the flow conditioning section of the HSWT (b) Detail view of high-visibility sight gauge

A quarter of the tank volume remains unfilled, allowing the free surface of the water to fluctuate within the tank. The tank is equipped with four threaded ports of various sizes used to connect an inlet, outlet, and two fluid-level sight gauges. High-visibility sight gauges with a floating bead (Fig. 3.7b) are used to monitor the water level from the mezzanine or lab floor. Schedule 40 PVC pipe connects the riser tank to the tunnel Fig. 3.8a) and a

manifold to the side of the contraction (Fig. 3.8c). The piping, sight gauges, and retention tank all include a factor of safety over twenty. The factor of safety is relative to 25.3 kPa (0.25 atm), which is the maximum additional static pressure that can be imposed on the HSWT.

The riser tank is connected to the tunnel at the top viewport, where air bubbles collect during filling and operation (Fig. 3.8a). In this arrangement, the riser tank automatically and continuously removes air from the tunnel without the need for manual venting. The manifold used for venting and pressurization is accessible from the mezzanine (Fig. 3.8c). A pressure gauge is installed in a highly visible location just above the contraction (Fig. 3.8b) for pressure monitoring during pressurization and throughout experimentation.

(a) (b) (c)

Figure 3.8: (a) Riser tank connection to tunnel at top viewport (b) Pressure gauge installed above contraction (c) Manifold with a vent and compressed air connection

A two stage valve system is implemented to prevent accidental overpressurization of the tunnel if an underregulated air source is connected to the manifold. The ball valve is used to engage or disengage the air source, while the trigger valve gives the operator fine control over the air flowing into the riser tank (Fig. 3.8c). To protect against improper pressurization, the vent valve is left open at all times except when pressurization above atmospheric pressure is necessary for an experiment.

Pressure regulation is also used to manipulate the dissolved gas content within the water column [8]. Air pockets trapped during filling of the HSWT are purged using the procedures outline in [6]. Air bubbles persisting after deaeration may be confused with cavitation; however, cavitation can only occur when the pressure of the liquid reaches its vapor pressure. It is rare that water tunnels are able to achieve a flow velocity high enough to cause the pressure of the test section to drop below the vapor pressure of water. However, it is common to see localized cavitation as the test section pressure drops with increasing velocity and the potential of caviation increases. The potential for a flow to cavitate is characterized by the cavitation number (Eqn. 3.1) where ρ is the density of the fluid, p is the local pressure, p_v is the vapor pressure of the fluid, and v is the net flow velocity. The pressure drop across test articles experiencing flow separation, for example, can reduce the local pressure enough to fall below vapor pressure and induce localized cavitation.

$$Ca = \frac{p - p_v}{\frac{1}{2}\rho v^2} \tag{3.1}$$

The duration and size of the bubbles observed in HSWT indicate that they result from dissolved gases coming out of solution. In accordance with Henry's law, which states that the amount of dissolved gas in a liquid is proportional to its partial pressure in the gas phase, as the pressure of the test section decreases, gas is forced out of solution and becomes visible. During qualification of the HSWT, air bubbles decreased the performance of laser-based instrumentation systems such as laser-doppler velocimeters (LDVs) by scattering or interrupting the laser beams used to track seeding particles through the water.

As mentioned previously, riser tanks can be used to mitigate the issues surrounding dissolved gases. Tunnels equipped for pressures above atmosphere can impose additional static pressure to keep the gas in solution. However, this method may conflict with pressure requirements for intentionally induced cavitation. Tunnels equipped for pressures below atmosphere

can induce sub-atmospheric pressures to remove dissolved gases prior to experimentation [8]. The HSWT is limited in its ability to control the solubility of dissolved gases due to its designed pressure range. However, facilities such as the Large Cavitation Channel (LCC) use a degassing system separate from the tunnel itself [3]. Packed-column degasification is one such method that can be used to degas water separately from the tunnel [9].

3.2.3 Results and Discussion

The riser tank has been installed since September 2018 and functions as designed with few exceptions. The floating balls inside the sight gauges failed within a month of installation, making it challenging to gauge the water level in the riser tank. A magnetic level indicator will replace the sight gauges. One phenomena not foreseen is the formation of vacuum pressures during draining as the water volume in the riser tank empties into the tunnel. The phenomena is explained by the differences in pipe size and elevation between the outlet of the riser tank and the outlet of the water tunnel. The outlet of the riser tank is located at the top of the water tunnel (Fig. 3.8a), and the outlet of the water tunnel is located approximately 3 m (9.84 ft) below the riser tank. Because of the difference in hydrostatic pressure between these two locations, the water tunnel drains faster than the riser tank and forms sub-atmospheric pressures in the HSWT. This effect is amplified by the 6.35 mm (1/4") difference in pipe diameter, with the water tunnel outlet being the larger of the two. Based on observation, the riser tank fully drains before immediate structural damage is inflicted. However, to prevent fatigue damage, operators are encouraged to slow the drainage rate by reducing the motor speed to 25% of the maximum flow rate or less until the riser tank is fully drained.

3.3 Pneumatic Hammer

Prompted by a hydroelastic damping experiment, a device was created to excite test articles in the HSWT for collection of vibration response data. An original solution was achieved through the use of a pneumatic double-acting air cylinder as detailed in this section.

3.3.1 Design Goals

Test article excitation within a water tunnel as been achieved with spark plugs and electromagnets [10]. However, it was determined that these solutions would pose unnecessary danger to the user, cause flow disruption, and interfere with measurement equipment. To allow spark plugs to fire underwater, voltages in excess of 4kV are required [11], which poses a significant safety hazard to the operator. Electromagnets have a short effective range relative to the size of the HSWT test section. Electromagnets powerful enough to act outside the test section are likely to create undesirable electromagnetic interference with instrumentation. Placing electromagnets within the test section decreases flow quality and requires waterproof electronics. The proposed design requirements for an alternative method are outlined in Table 3.3.

Design Goal	**Description**
Flow Speed	Must withstand the fluid forces imposed up to 10 m/s
Minimal Flow Disturbance	Minimal impact on flow surrounding test article
Adjustable and Repeatable Force	Impact force must be controlled and repeatable
Modular Design	Maximize use of standard parts
Vibration Isolation	Excitement of structures other than the test article should be minimized
User Friendly	Final design must minimize the time needed to conduct research with easy installation and a user interface
Safety	Device should minimize the safety risks to users, particularly the use of high voltage electricity near water

Table 3.3: Pneumatic hammer design requirements

.

3.3.2 Design Process

As an alternative to spark plugs and electromagnets, an actuator with an extendable rod is used to strike test articles. The actuator extension rod (Fig.3.9a) rapidly extends into the test section at the press of a button and immediately retracts up into the aluminum top plate out of the flow. While electric actuators provide a predictable striking force and fast actuation time, they carry a higher risk of electrical shock and are more costly than pneumatic air cylinders. Electric actuators also lack a threaded nose for mounting the actuator to the aluminum top plate. Thus, a standard round-body air cylinder was chosen as the actuator for construction of a pneumatic hammer. The concept of operation for a double-acting cylinder is detailed in Figure 3.9.

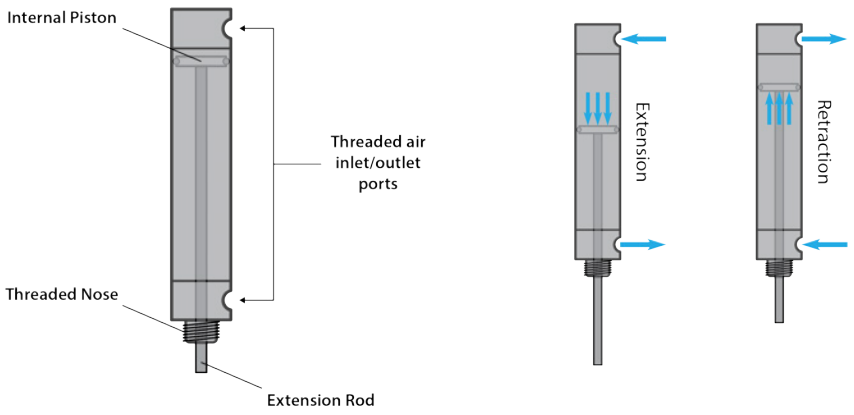

Figure 3.9: (a) Annotated illustration of a round body double-acting air cylinder (b) Illustration of the actuation cycle for a double-acting air cylinder

To size the extension rod of the cylinder, a bending moment calculation was performed to ensure the extended rod would withstand fluid drag forces up to 10 m/s (32.8 ft/s). Based on rod sizes and materials available for commercial purchase, a model was developed using a 6.35 mm (0.25") diameter 304 stainless steel rod extending to the centerline of the test section (152 mm, 6").

The extension rod is modeled as a cylinder in cross flow where ρ is the density of the water, U is the test section velocity, l is the length of the rod exposed to the flow, D is the diameter of the rod, and μ is the dynamic viscosity of water at room temperature. The Reynolds number, Re, for the rod at 10 m/s (32.8 ft/s) was calculated to be approximately 57,000 using Equation 3.2 below. Equation 3.3 was used to find the drag force, F_D, with an estimated maximum drag coefficient, C_D, of 1.25 [12].

$$Re = \frac{\rho U D}{\mu} \tag{3.2}$$

$$C_D = \frac{F_D}{\frac{1}{2}\rho U^2 D l} \tag{3.3}$$

The resulting drag force, F_D, on the extension rod is 60.5 N (13.6 lbf). The maximum bending stress of the rod can be calculated using Equation 3.4 below:

$$\sigma_{b,max} = \frac{Mc}{I_c}, \tag{3.4}$$

where M is the bending moment at the location of interest along the rod length, I_c, is the centroidal moment of inertia of the rod's cross section, and c is the distance from the neutral axis to the outermost fiber. The force F was assumed to act at distance, x, equal to half the length of the rod (62mm, 3").

$$M = Fx \tag{3.5}$$

$$I_c = \frac{\pi D}{16} \tag{3.6}$$

Equations 3.4-3.6 resulted in a maximum bending stress of 183 MPa (26600 psi), yielding a 1.2 factor of safety based on the a yield strength of 221 MPa (32100 psi) [1].

Based on calculations and commercial availability, a 1-1/16" bore pneumatic air cylinder was selected with a 6.35mm (0.25") rod diameter, 203 mm (8") stroke length, and 3/4"-16 threaded nose for attachment to the aluminum top plate discussed in Section 3.1. As mentioned previously, a stroke length of 152 mm (6") is needed to reach the centerline of the test section. The additional stroke length extends the moment arm between the piston head and the cylinder nose to counteract the moment arm imposed by drag forces. The nose is equipped with a dynamic seal that allows the rod to translate in and out of the cylinder while retaining air pressure within the cylinder. A double-acting air cylinder is used for independent control of extension and retraction as shown in Figure 3.9b. At each threaded inlet, a 1/8" NPT nipple connects a 3-way, 3-port, normally-closed solenoid valve.

A waterproof electronics enclosure houses a microcontroller and supporting electronics. To create a user interface, the face of the electronics box was modified to mount an LCD screen, potentiometer, and three switches (Figure: 3.10a). A small circuit board connects the solenoid valves to TIP 120 Darlington transistors, allowing the lower voltage microcontroller signals to trigger the higher voltage solenoids (Fig. 3.11).

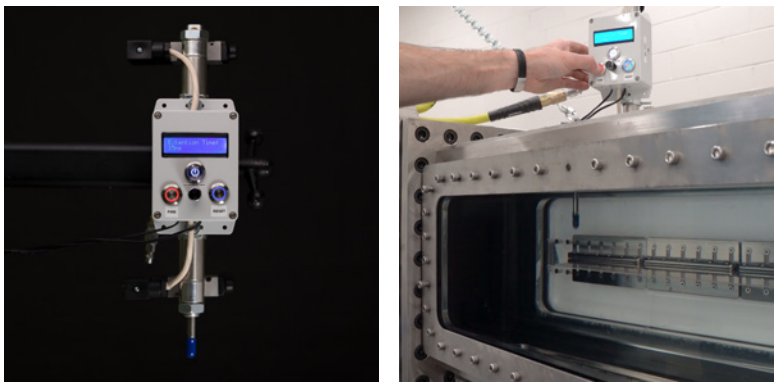

(a) (b)

Figure 3.10: (a) A close-up of the assembled pneumatic hammer. (b) The pneumatic hammer attached to the aluminum top plate with rod extending into the flow.

The electronics box is attached to the air cylinder using conduit pipe clamps. The microcontroller is programmed to control the extension and retraction of the rod based on the activation time of the solenoid valves. The potentiometer allows the user to control the extension length of the rod, based on the amount of time the top solenoid valve is opened. The extension time is displayed on the LCD screen in milliseconds. The micro-controller is programmed to have a retraction time twice as long than the extension time to ensure that the rod will fully retract. In the event that the rod does not fully retract, a reset button is installed that returns the rod to a fully retracted position. A full schematic of the electronics for the pneumatic hammer is provided in Figure 3.11. For installation on the aluminum top plate, an o-ring is fitted at the base of the 3/4"-16 threaded nose (Fig: 3.9a) and the assembly is screwed into a port on the aluminum top plate. A rubber cap is attached to the tip of the rod to protect test articles from damage when struck.

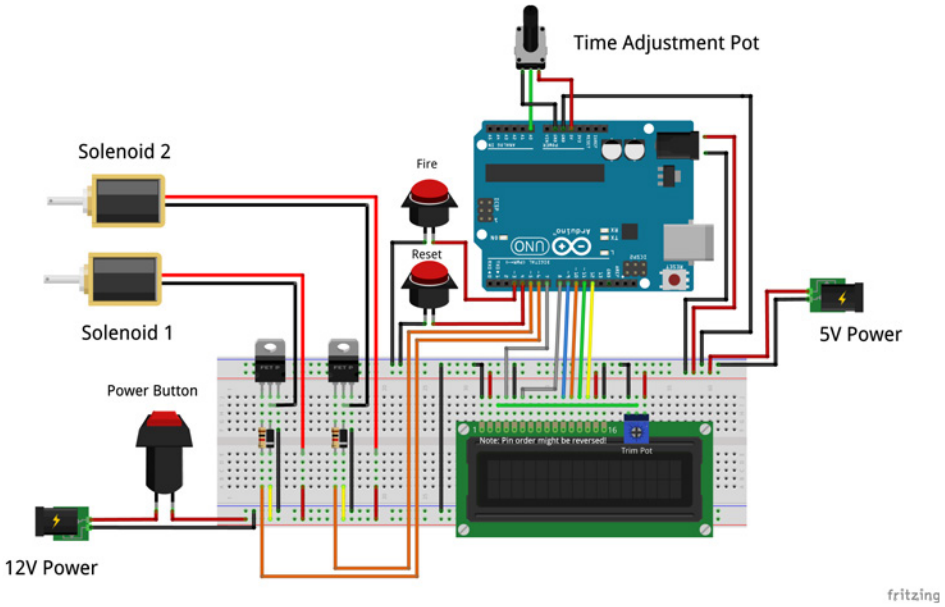

Figure 3.11: Fritzing diagram of the pneumatic hammer electronics

3.3.3 Final Design and Testing

Since construction, the pneumatic hammer has been used to yield novel results in hydroelasticity experiments involving flat plates [13]. As these experiments progressed, the pneumatic hammer's impact on flow quality was explored. Experiments were carried out using a high-speed camera and the dye injection system discussed in Section 4.3. The tip of the extension rod was placed statically against a plate to observe vortex formation at the rod tip (Fig. 3.12).

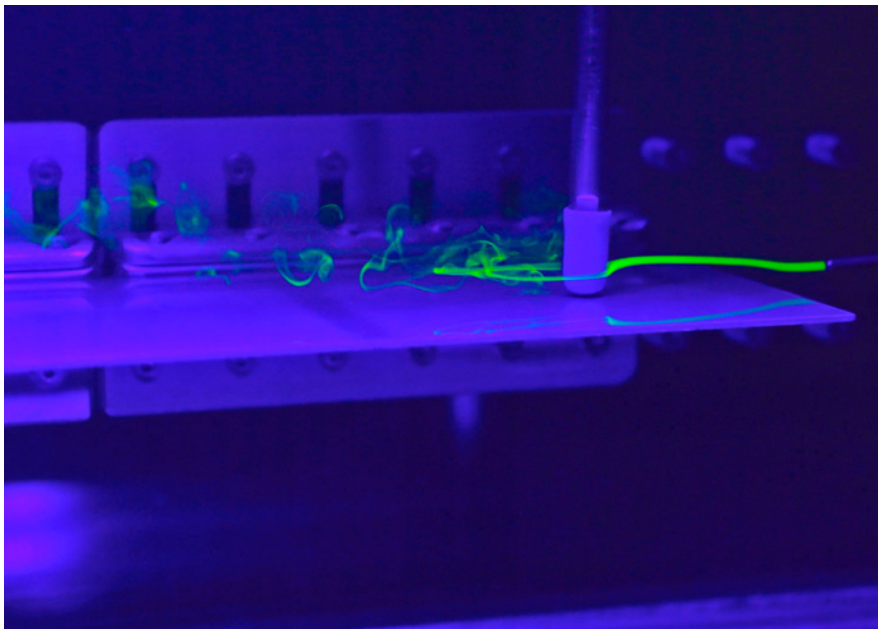

Figure 3.12: Vortex shedding around the extension rod of the pneumatic hammer

Next, a dynamic test was performed to study the duration of the vortex formation after the rod has struck the test article. The high-speed camera revealed that the hammer tip impact is under 1/60th of a second (17 ms), limiting the time available for vortex formation near the plate. When the hammer tip is positioned to strike on the downstream end of the plate, vortices are swiftly carried off the end of the plate. The duration of fluid disturbances caused by the vibration of the plate after impact far exceeded the duration of disturbances caused by the hammer tip (Fig. 3.13). At a flow velocity of 0.1 m/s (0.33 ft/s), the velocity

used for these dye injection tests, the flow disturbances caused by the vibrating plate exceeded the flow disturbances caused by the hammer by a factor greater than fifteen. This factor is not expected to decrease as flow velocity increases. While the intensity of the vortices shed from the extension rod will increase with flow velocity, they will also be carried away from the plate at a greater velocity. These experiments demonstrate that while the pneumatic hammer does impact flow quality, the impact can be minimized through short actuation time and strategic placement of the impact location. The time history of the vibration data collected for the flat plates did require truncation to exclude the impact of the hammer tip.

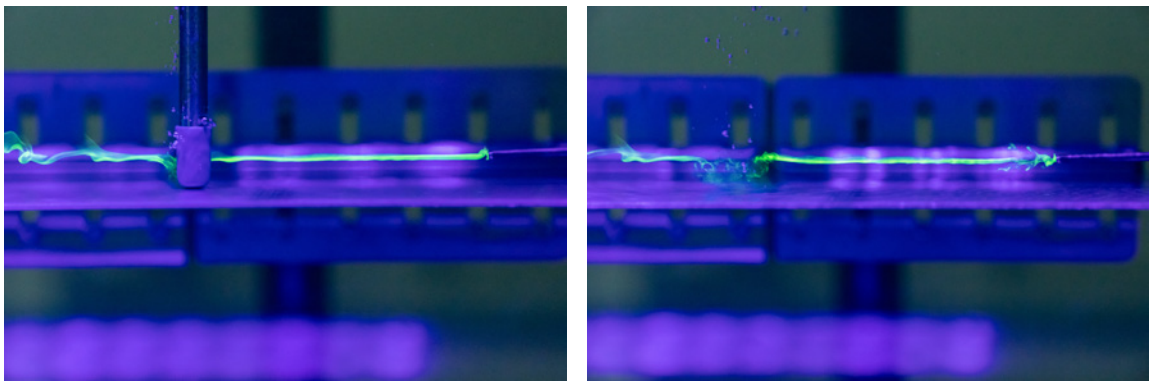

(a) (b)

Figure 3.13: (a) Flow visualization of the pneumatic hammer tip as it impacts a flat plate (b) The dye stream 1/10th of a second after hammer impact. Note that the flow disturbances seen a the dye injection nozzle on the right are caused by the vibration of the plate after impact.

The ability to collect force data at the tip of the rod is desired for modal testing. Attempts to estimate the impact force of the rod tip have not been successful. Testing for hydroelastic damping was completed without force data by using the log-decrement method. For future iterations of this system, the ability to acquire force data upon impact remains a high priority.

User feedback indicated a need to use a cushioned air cylinder and to improve the mobility of the hammer unit. The impact force of the piston retracting interfered with vibration measurements, which can be addressed with a cushioned air cylinder designed to absorb the

impact force. Although compact in form, locating the control box and solenoids directly on the air cylinder makes it cumbersome to install on the aluminum top plate and requires that the user be within arms reach of the test section. Often the user is stationed away from the test section, and with most experiments requiring hundreds of tests it was requested that a remote firing mechanism be provided for convenience. The next iteration of the pneumatic hammer will centralize the user interface and solenoids into a single unit that is detached from the cylinder itself. Push-to-connect tubing adapters will be placed on the air cylinder so that the tubing can be detached for unrestricted installation and removal of the cylinder. This will also allow the cylinder to be installed in all hole locations on the aluminum top plate, whereas interference with the plugs and bottom solenoid currently permit the pneumatic hammer to be installed at outer hole locations.

The design of the dynamic seal within the cylinder nose presents two challenges that require further experimentation to solve. At flow velocities nearing 10 m/s (32.8 ft/s), the friction in the piston is increased due to the moment caused by fluid drag forces, and a higher pressure is typically required to successfully operate the pneumatic hammer at flow velocities nearing 10 m/s (32.8 ft/s). This may be remedied by oversizing the stroke length more than discussed previously. When the water tunnel is pressurized, water leaks into the cylinder and out through the solenoid valves. As the flow speed of the tunnel increases and the pressure in the test section decreases, this problem is temporarily mitigated. A pneumatic air cylinder may not be suitable for tunnels pressurized above 127 kPa (1.25 atm). A standard air cylinder has not yet been identified with dynamic seal characteristics suitable to resolve these challenges and a custom design may be required.

3.4 Test Section Traverse

Experiments involving flow visualization often require the mounting of lighting equipment and dye injection fixtures over the test section. To accommodate such equipment, a traverse system was created using 80/20 rail, also known as extruded t-slot aluminum. A bracket was fabricated to allow the side rails to run the length of the test section, using the flange bolts as anchor points (Fig. 3.14a). The mounting bracket allows for quick installation and removal of the railing system without having to disassemble the rail system for each use.

A double railing mounted to a pair of rail carriages (Fig. 3.14b) spans the width of the test section, allowing equipment to be traversed directly over the test section (i.e. the dye injection system discussed in Sec. 4.3). The railing can also be used in combination with a friction arm, commonly used for camera equipment, to mount lights and cameras around the test section. Friction arms are also be used to secure instrumentation passed through the aluminum top plate, such as CTA probe supports.

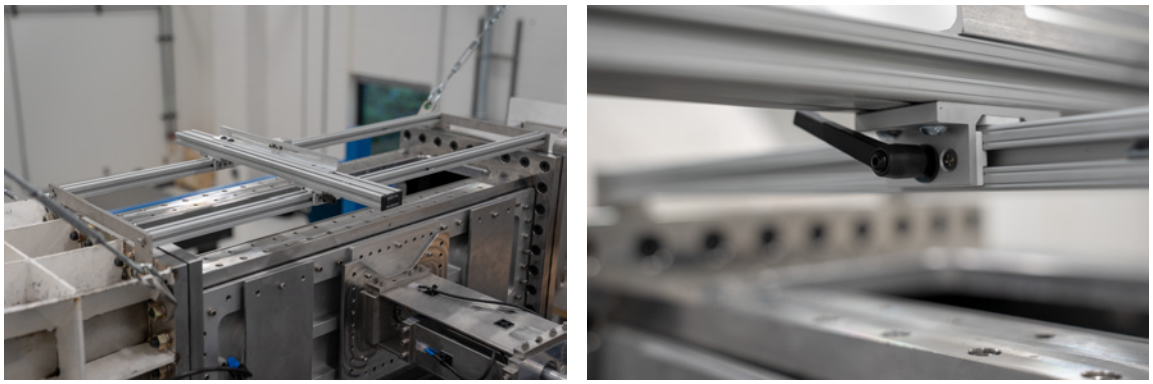

(a) (b)

Figure 3.14: (a) Test section traverse attached to test section (b) Detail view of rail carriage

3.5 Safety Mesh

In designing the HSWT, sizing and budgetary constraints prevented the installation of access ports over the downstream turning vanes and the propeller. Access ports strategically placed in these locations enable direct removal any foreign objects in the tunnel without the need to disassemble the tunnel. Because access ports were not installed, a safety bracket (see Fig. 3.15) was designed to secure on the downstream side of the 'breadboard' window described in Section 3.1. The bracket incorporates a stainless steel frame and 6.35 mm (1/4") square mesh welded to the frame.

Figure 3.15: The safety bracket designed to fit within the test section and catch stray test articles.

Although the bracket is structurally designed to withstand the fluid forces up to 10 m/s, the bracket creates a blockage in the test section large enough to result in pump cavitation below speeds of 5 m/s. The blockage ratio can be calculated by dividing the frontal area of the object in the test section by the cross-sectional area of the test section. The blockage of the safety bracket is approximately 30% of the cross-sectional area of the HSWT test section. The maximum blockage for a water tunnel depends on multiple factors including test section geometry and pump design. A maximum blockage ratio of approximately 30% is common in high speed water tunnels [2]. The mesh on the bracket also creates audible flow

induced vibration in flow speeds over 1 m/s. Hence, the safety bracket has been relegated to low-speed experiments below 2 m/s. The bracket has been used as a filter, placing aquarium filter mesh on the upstream side of the frame. This is an effective method for removing debris too large for the filter system (Sec. 5.1), such as silicone chunks from construction. Alternative methods for the containment and collection of stray test articles at high flow speeds are still being explored.

Chapter 4

Instrumentation

There are three types of water tunnel instrumentation that were assembled in-house including a flow meter, force balance, and two dye injection systems. This chapter outlines the design and purpose of each instrument and provides an account of their performance characteristics. For further details on commercial water tunnel instrumentation, refer to [6].

4.1 Flow Meter

For the first year operation, the test section velocity of the HSWT was estimated based on a relationship between the motor drive frequency and the center velocity of the test section as measured by an LDV system during qualification. This method is known to introduce irregular error in flow rate estimations due to belt slippage discussed in Section 5.3. A solution was devised using the Venturi effect — the reduction in fluid pressure that results when a fluid flows through a constricted section of a pipe. In this case, the pressure drop across the contraction is used to estimate the flow velocity of water entering the test section. Because there is no elevation change across the contraction, a simplified version of the energy equation from fluid mechanics (Eqn. 4.1) was used to derive the velocity

relationship in Equation 4.2 below where P is pressure, v is velocity, A is cross-sectional area, and ρ is fluid density. For this calculation, the subscript '1' denotes the characteristics of the upstream side of the contraction, and the subscript '2' denotes the characteristics where the contraction connects to the entrance of the test section.

$$P_1 + \frac{1}{2}\rho v_1^2 + \cancelto{0}{\rho g h_1} = P_2 + \frac{1}{2}\rho v_2^2 + \cancelto{0}{\rho g h_2} \tag{4.1}$$

$$v_2 = \sqrt{\frac{2\left(P_1 - P_2\right)}{\rho\left[1 - \left(\frac{A_2}{A_1}\right)^2\right]}} \tag{4.2}$$

4.1.1 Design Goals

A list of design requirements for the flow meter are summarized in Table 4.1.

Design Goal	**Description**
Non-Invasive	Flow meter should not induce significant disturbance in the boundary layer of the test section
Multi-Purpose	Pressure sensor should be useable for multiple purposes such as pitot tubes, pressure drop analysis around the tunnel, and other pressure measurements around the tunnel
Accuracy	Mean flow velocity should be measured within 2% accuracy
Blockage	Significant error should not be introduced when test articles block
Waterproof	Pressure sensor must be designed for continuous use with water, and resistant to corrosion in the presence of 304 stainless steel
User-Friendly	Pressure sensor should LabVIEW compatible and require little training to use for research

Table 4.1: A summary table of design requirements for the flow meter

.

4.1.2 Selection Process

A variable reluctance differential pressure transmitter (Validyne, P55D-1-N-1-42-S-3-A) was selected as the data collection device (Fig. 4.1) for the flow meter. The transmitter is constructed from stainless steel to resist corrosion, and is designed to accept both gases and liquids directly at the sensing diaphragm [14]. The sensing diaphragm is exchangeable, allowing for increased accuracy in specific pressure ranges. To select the correct diaphragm, Equation 4.1 was used to estimate the pressure drop across the contraction. At a test section velocity 12 m/s (39.4 ft/s) the estimated pressure drop across the contraction is approximately 97.9 kPa (14.2 psi). A 138 kPa (20 psi) diaphragm was selected to provide a factor of safety against diaphragm rupture and for versatility of application.

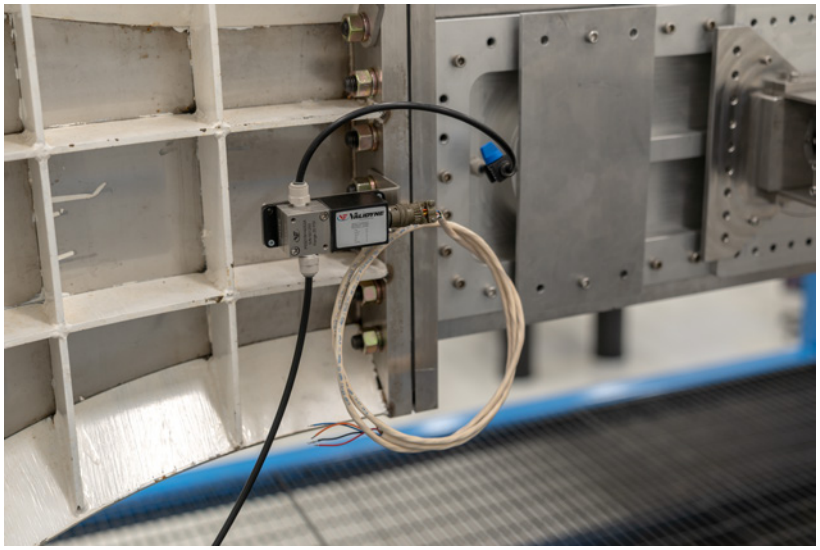

Figure 4.1: The differential pressure sensor mounted on the side of the contraction.

A custom bracket mounts differential pressure transmitter near the test-section as displayed in Figure 4.1. Pressure taps located in various locations around the water tunnel, including a tap upstream of the contraction, were pre-installed during the fabrication of the HSWT. As noted in Section 3.1, a pressure tap is mounted along the centerline of an acrylic window and the aluminum force balance window. Each pressure tap is mounted such that

the face is flush with the inside of the window to minimize flow disturbance in the test section. It should be reemphasized that metal pressure taps are not recommended for use with acrylic window, as they have a tendency to split and crack the acrylic window over time.

4.1.3 Results and Discussion

Unexpected delays in the rental of an LDV system prevented the flow meter from being fully calibrated by the time of publication. The objective is to map a relationship between the centerline velocity of the test section and the voltage reading from the differential pressure sensor. If calibrated in this manner, the accuracy of the flow meter would be within 0.7% as the accuracy of the pressure sensor is 0.5% [14] and the accuracy of the LDV is 0.2% [15]. Additional tests are scheduled to identify potential sources of measurement error. Pre-identified grounds for testing included the effects of pressure tap orientation within the test-section, effects of electromagnetic interference on the transmitter, boundary layer effects, and the blockage caused by test articles in the test section.

Figure 4.2: One of six pressure taps installed on the HSWT with a removable plug

The six pressure taps located around the tunnel structure are outfitted with push-to-connect adapters (See Fig. 4.2) to serve as measurement points for the differential pressure sensor. To corroborate the true operating limits of the tunnel, this data will be compared

to the theoretical flow-loop analysis used to design the structure of the water tunnel. When calibrated the flow meter will serve to accurately measure test section velocity, quantify energy losses in the tunnel, and provide a source of data verification while using systems such as LDVs.

4.2 Force Balance

The ability to measure fluid forces imposed on a test article is critical for hydrodynamic characterization. An existing force balance design for water tunnels was sourced from the University of New Hampshire (UNH) [16], and modified to fit the specific needs of the Dynamic Devices and Solutions Lab. The original force balance is equipped to handle test lift loads of up to 960.8 N (216 lbf) and drag loads up to 22.2 N (5 lbf). A brief summary of the force balance operation principles and modifications are as follows.

As displayed in Figure 4.3, test articles are secured to one end of the hydrofoil rod using a key and slot while the other end of the rod is passed through a radial flex seal (Fig. 4.4a) and clamped to a series of bending plates. The plug and front plate are used to attach the fully assembled force balance into a window designed to mate with the force balance plug (Fig. 4.4b). Fluid forces imposed on test articles cause small deflections of the hydrofoil rod, which deforms the bending plates. Strain gauges applied to the bending plates convert the deformation of the plates into an electrical voltage signal, which is scaled to reflect the load imparted on the test article based on an empirically derived calibration curve.

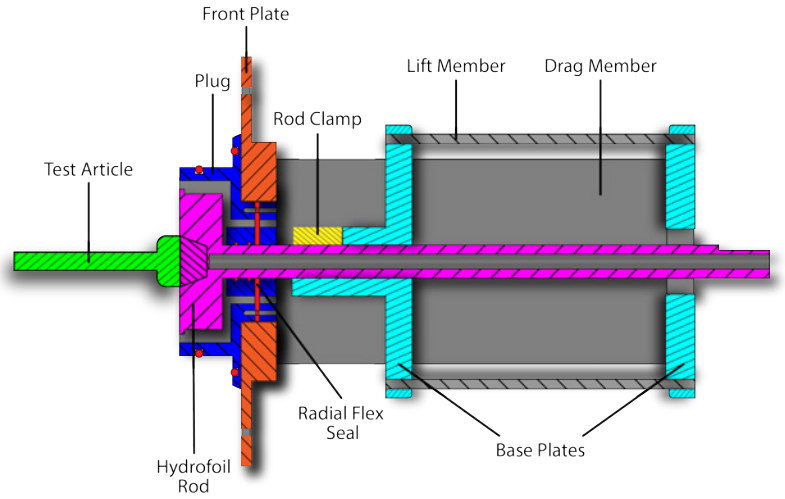

Figure 4.3: Section view illustration of the force balance displaying the primary assemblies

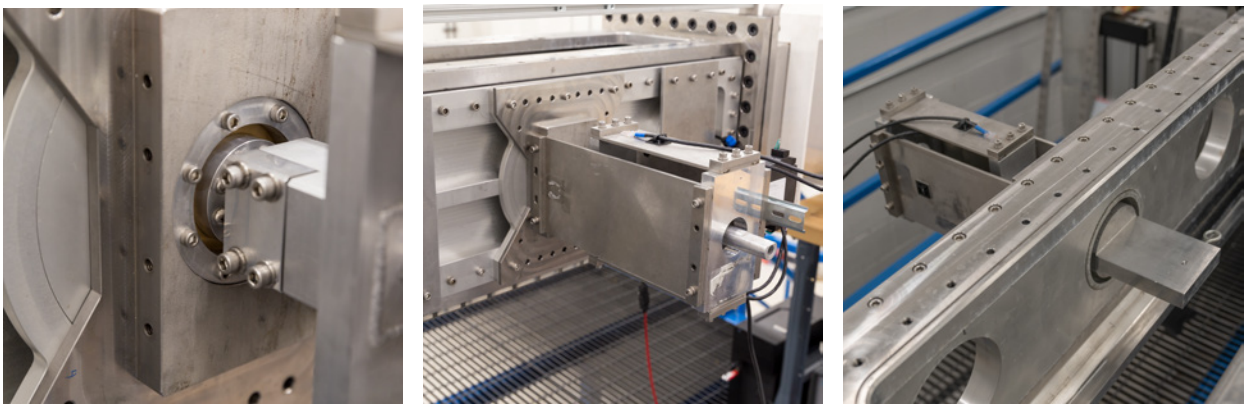

(a) (b) (c)

Figure 4.4: (a) Radial flex seal and clamp inside of the force balance assembly (b) Assembled force balance inserted into an aluminum window (c) Isometric view of force balance attached to test section

4.2.1 Design Modification Goals

Based on the known operating limits of the force balance design provided by UNH, a list of modification objectives are summarized in Table 4.2.

Design Goal	**Description**
Resizing	Appropriate components of the force balance should be modified and sized to fit the HSWT
Rigidizable	Force balance should be allow for rigid mounting without force measurement
Versatility	Signal conditioner should be multipurpose

Table 4.2: Summary of force balance modification goals

4.2.2 Design Process

A computer aided design (CAD) model was generated from the drawings provided by UNH, which was modified to meet the requirements listed in Table 4.2. The front plate, which attaches the force balance to the test section, is scaled to fit the relatively larger test section, and the screw holes are resized appropriately. The plug and hydrofoil rod are lengthened to account for the increased thickness of the HSWT test section windows. The universal mounting slot and key are modified to have a 7° taper to increase rigidity, waterproofing, and ease of machining. To reduce cost, many of the original stainless steel components are fabricated from anodized aluminum. The bending plates are fabricated from 304 stainless steel versus 410 due to material cost, availability and machinability. Based on the desired material properties outlined in [16], exchanging stainless steel grades was not expected to adversely affect the performance of the force balance.

To allow the hydrofoil rod to be rigidized, a retaining ring was made from PVC designed to lock the hydrofoil in place while still allowing the rod to rotate (Fig. 4.5). An o-ring and groove designed for a dynamic piston-type seal is placed around the outside diameter

of the retaining ring to create a slight interference fit for increased rigidity. A 3.175 mm (1/8") deep shoulder is cut into the outward face of the retaining ring to ensure that the face plate will remain flush with the wall of the test section. The shoulder serves as as the contact point where the hydrofoil rod is held in place. Due to the tight fit required to fix the retaining ring within the plug, precautions were taken to make the retaining ring easily removable. Two threaded holes were placed on opposite sides of the retaining ring to allow long screws to be inserted and push the retaining ring outward.

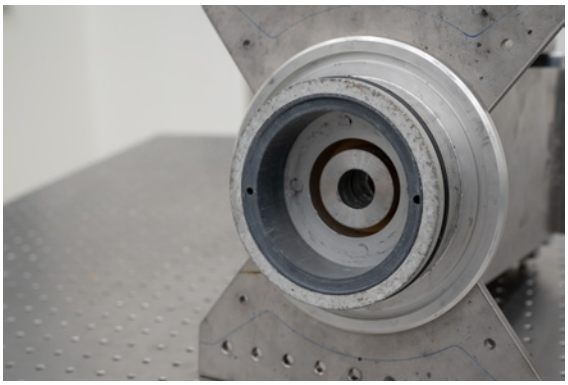

Figure 4.5: PVC retaining ring used to rigidize the force balance

Despite their widespread use in structural testing and monitoring applications, strain gauges are one of the most difficult types of sensors to use due to signal conditioning challenges including electrical noise, temperature fluctuations, and improper calibration [17]. A commercially produced strain gauge signal conditioner (Omega, DMD4059) is used with the force balance. Desired characteristics for a signal conditioner include an adjustable excitation voltage, directly adjustable offset, and resistance to electromagnetic interference (EMI). Adjustable excitation voltage can be used to optimize the signal-to-noise ratio from the strain gauges and reduce errors caused by self-heating [17]. In addition, an adjustable excitation allows for a wider variety of applications. Voltage offset is used to compensate for imbalances in the strain gauge bridges, such as small manufacturing variations or preloading of the strain gauges.

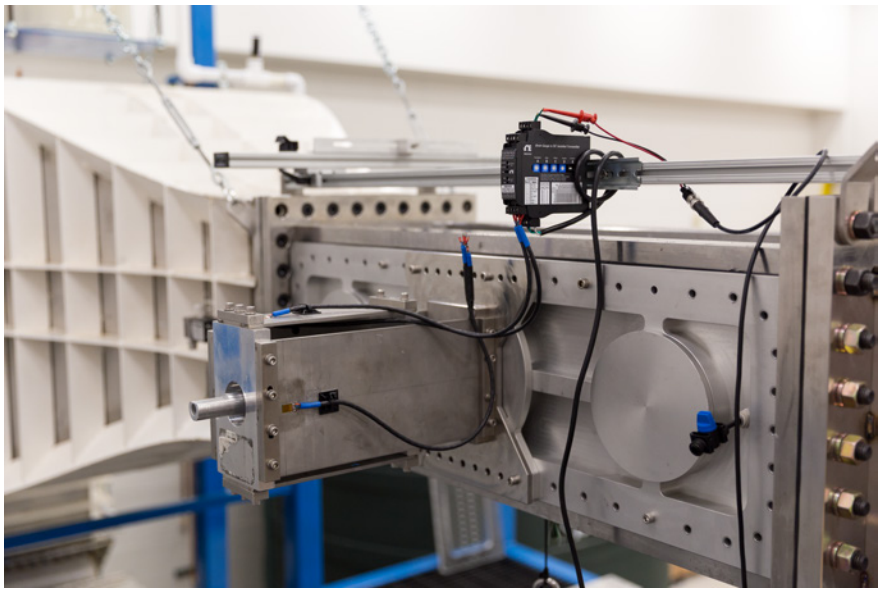

Figure 4.6: Signal conditioner attached to 80/20 railing using a standard 35mm DIN rail

During initial experimentation with strain gauges, it was discovered that the electric motor driving the HSWT introduced significant electrical noise. The signal conditioner selected incorporates an EMI resistant circuit design; however, additional steps were taken to promote EMI resistance. The lead wires from the strain gauges were kept to a minimum length, and a shielded cable (Magnetic Shield Corp.,Inter-8 Weave) connects the strain gauges to the signal conditioner [18]. The cables soldered to the strain gauges are secured using bridge terminal pads and cable tie anchors (Fig. 4.7a) to prevent accidental detachment of the strain gauges and provide strain relief for the cable. A protective layer of silicone was placed over the strain gauges. Ferrules are used to connect the leads of the strain gauge cables and provide a reliable connection to the terminal blocks of the signal conditioner. As detailed in [16], a full-bridge strain gauge configuration is used.

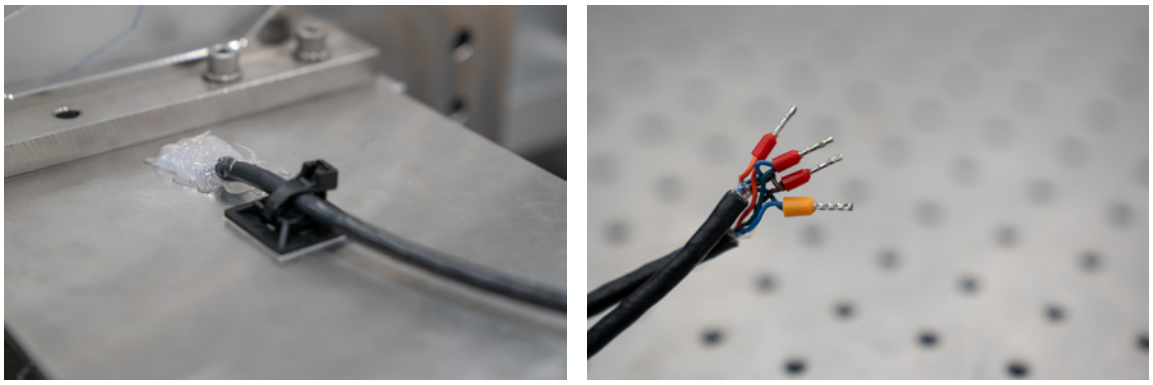

(a) (b)

Figure 4.7: (a) Cable-tie anchors and silicone used to protect the strain gauges (b) Ferrules used to connect the strain gauge leads

4.2.3 Results and Discussion

The force balance is calibrated using a range of weights applied in the lift and drag direction using the calibration tool designed to simulate a hydrofoil (Fig. 4.9a). Calibration establishes a relationship between the load applied to the force balance and the output voltage from the signal conditioner. To develop a calibration curve, a series of multiple loads are applied by placing weights in a bucket suspended by the calibration tool. The signal conditioner is allowed 2-3 minutes to warm up before taking measurements, and the initial voltage is offset to zero once the readings have stabilized. To verify repeatability, measurements are collected for each load during both loading and unloading often with multiple trials. The relationship displayed in Figure 4.8 is only valid for a specific signal conditioner configuration and directly depends on the selected excitation voltage, input range and output range. The calibration results displayed in Figure 4.8 were collected using a 5V excitation voltage, input range of 0-5 mV, and output range of +\- 5V.

Calibration of the modified force balance revealed a lift force sensitivity of 8.11 mV/N (36.1 mV/lb) and a drag force sensitivity of 7.69 mV/N (34.2 mV/lb). The output voltage

value is scaled to the corresponding force value by dividing over the sensitivity. The calibration coefficient is subject to change due to thermal expansion effects and pretensioning of the bending plates. The force balance is recalibrated before each experiment and following any changes to the plate assemblies. During initial calibration several sources of error were identified and address including the calibration pulley, radial flex seal, and electromagnetic interference.

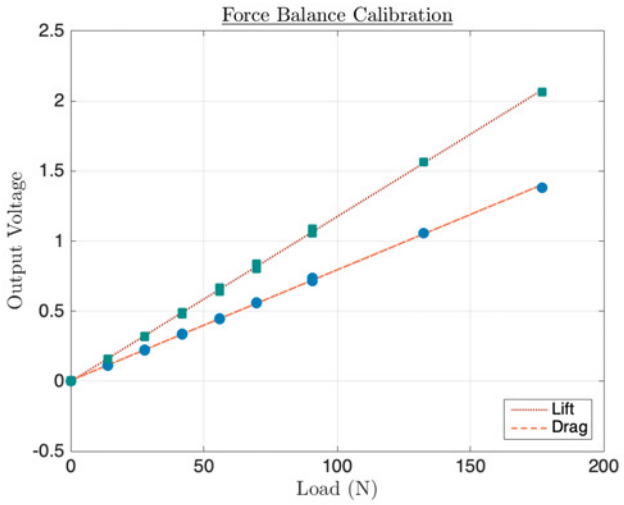

Figure 4.8: Force balance calibration curves with a linear fit

The pulley system originally designed to simulate a drag load caused inconsistencies in the voltage measurements. Despite efforts to use different types of rope and reduce friction, the pulley system did not deliver a consistent load to the calibration tool. One of the phenomena observed is a gradual drift in the measurement over several minutes, attributed to the elongation of the string interacting with the pulley.

The mounting plate of the force balance was subsequently drilled and tapped to allow the force balance to be rotated 90 degrees (Fig. 4.9b). In the rotated orientation, weights are directly hung from the calibration tool for drag calibration. An added benefit of changing the orientation of the force balance is that the lift plates can be used to collect drag measurements up to 960.8 N (216 lbf) [16].

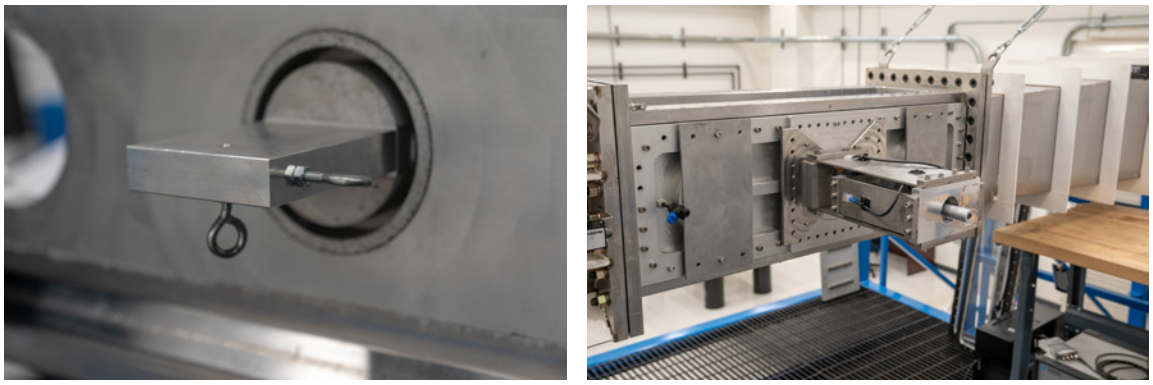

(a) (b)

Figure 4.9: (a) The calibration tool used to hang weights from the force balance. (b) The force balance rotated to simulate a drag load by suspending weights from the calibration tool.

During initial calibration the loading curve would become non-linear above 133.4 N (30 lbf). This is attributed to the radial flex seal bunching as it began to approach the outer flange ring of the seal assembly. The bunching of the seal will occur naturally as the force balance reaches its maximum load capacity; however, the rubber is also deformed from the clamping forces keeping the seal in place. The original seal design was modified to account for the deformation experienced during clamping. Using a waterjet for fabrication, both the inner and outer radius of the seal are trimmed by 0.7938 mm (1/32") to account for extrusion as the seal is clamped into place. The radius from the center of the seal to the outer ring of thru holes is reduced 0.7938 mm (1/32"), accounting for the hole displacement caused by extrusion during clamping. The modified seal design prevents premature bunching of the seal and restored a linear calibration curve up to 178 N (40 lbf) in both directions.

Despite the extensive measures taken to reduce EMI in the design of the strain gauge circuits, there is still a need to quantify the effects of various EMI sources in the operating environment. Namely, the electric motors that power the filter pump and the HSWT

propeller shaft. A series of preliminary tests were conducted to establish which of the two known EMI sources warranted further testing. For each test, three trials were completed by averaging 20 seconds of data collected at a sampling frequency of 1000 Hz. To test the effect of motor speed on EMI while not imposing a load on the force balance, the water level was drained just below the test article. The results of these tests are displayed in Figure 4.10 below:

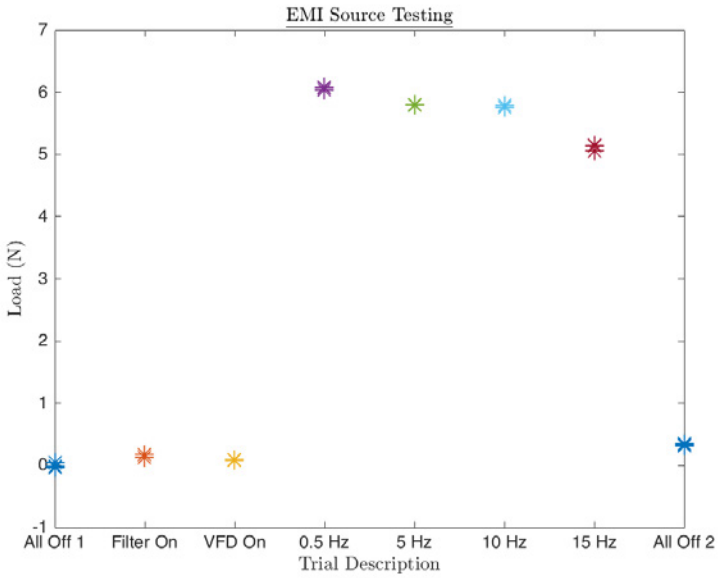

Figure 4.10: Variation in output voltage as EMI sources are placed into various configurations (frequencies are that of the motor drive)

Turning on the main motor results in an EMI induced artificial load of 3.11 N (0.7 lbf) based on the calibration curve shown in Figure 4.8. Once the motor is turned on, the maximum error between measurements is approximately 1 N (0.22 lbf), which is within the accuracy range of the original force balance [16].

To test the response time of the force balance to sudden load changes, a thin string connecting a 6 N (1.35 lbf) load to the calibration tool was cut to simulate an impulse load. The results of this experiment are shown below in Figure 4.11. The data was collected at 1000 Hz, and the impulse response of both channels is between 250ms to 300ms.

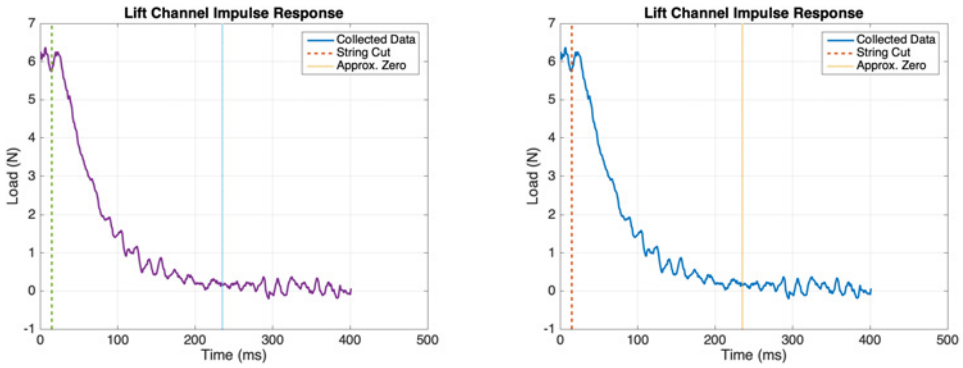

(a) (b)

Figure 4.11: (a) Force balance calibration tool (b) Calibration tool rotated to simulate drag load.

The scope of this thesis is limited to the modification, basic calibration, and error source identification of the force balance. Further testing will be conducted to assess and improve the capabilities of the force balance. This will include "cross-talk" testing between the lift and drag channels, and modal testing. The bending plates are not perfectly rigid in the direction opposite to which they measure causing a phenomenon known as "cross-talk" [16]. For example, if a pure drag load is applied to the force balance the lift members will experience a small deflection and register a false load in the lift direction. At the time of publication, only one signal conditioner has been procured, and therefore data can only be collected from one channel at a time. When a second signal conditioner is procured, it will be necessary to quantify a correction factor for both channels to account for cross-talk in experimental measurements. Modal analysis of the force balance will be necessary to distinguishing natural frequencies of the force balance from those of the test articles attached to the force balance. This testing can be carried out using a laser vibrometer or accelerometer. This list of tests is not exhaustive. To fully characterize and optimize the behavior of the force balance will require extensive use and testing, often specific to the experiment being conducted.

4.3 Dye Injection

The observation of fluid motion using dye is one of the oldest flow visualization techniques in fluid mechanics. This technique is inexpensive and easy to implement, and it offers significant insight into the phenomena occurring in complex fluid flows. Dye reservoirs can be gravity-fed or pressurized. Gravity-fed systems are inexpensive and straight forward to construct; however, a pressurized reservoir provides a more consistent flow rate and can be operated at higher speeds. This chapter outlines the construction of both a gravity-fed and pressurized dye injection system as well as many of the supporting tools needed to use these systems. A summary of design goal for the dye injection systems is provided in Table 4.3.

4.3.1 Design Goals

Design Goal	**Description**
Consistent Flowrate	Flowrate should remain consistent as reservoir depletes
Operating Range	Pressurized dye injection system should be capable of operating up to 3 m/s
Open and Closed Channel	One system should be operable in a closed channel configuration
Commercial Parts	Standard parts should be used for cost and repairability
Minimal Pollution	Dyes must be removable via filtration
User Friendly	Less than 20 minutes should be required for setup

Table 4.3: Design requirements for both a gravity-fed and pressurized dye injection system

4.3.2 Design: Gravity-Fed Dye Injection

The major drawback of a traditional gravity fed dye system is the decrease in flowrate as the reservoir is depleted. However, a constant head reservoir known as a Mariotte bottle, can be used to deliver the dye at a constant rate, even as the dye reservoir is depleted. A Mariotte bottle is sealed except for a vent tube, which extends very close to the bottom of

the reservoir. As the reservoir empties, air is drawn into the bottle to equalize the pressure, maintaining atmospheric pressure at the tip of the vent tube. The reservoir's head pressure is fixed relative to the distance between the bottom of the vent tube and the free surface below.

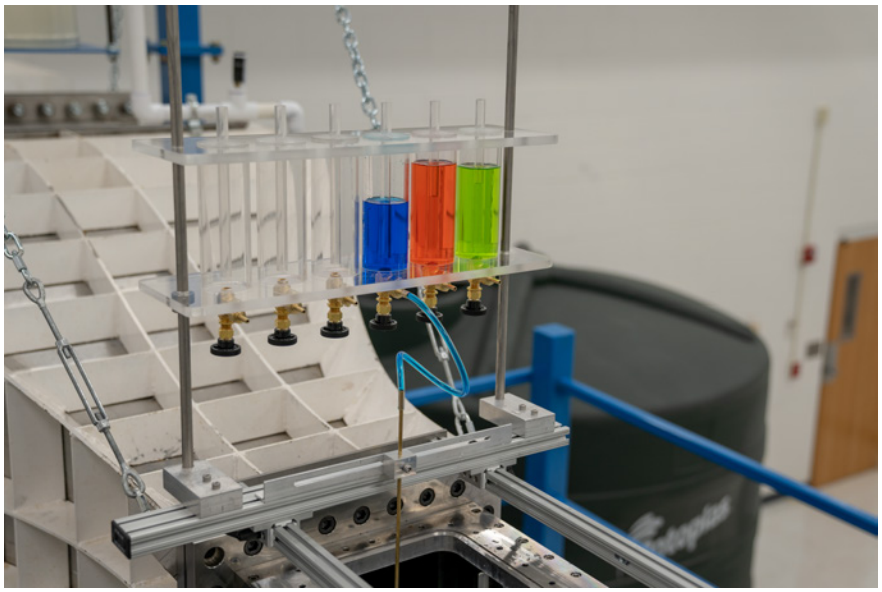

Figure 4.12: An overview of the gravity-fed dye injection system.

For simultaneous injection of multiple dye lines, six reservoirs are included in the design of the gravity-fed system (Fig. 4.12). Each reservoir is made of clear cast acrylic with a diameter of 50.8 mm (2") and a height of 203.2 mm (8"). Vent tubes are incorporated into the caps, each of which are outfitted with a piston-style o-ring for an air-tight seal. All six reservoirs are attached to a double platform assembly which is designed to slide up and down 12.7 mm x 914 mm (1/2" x 36") rods to adjust the head pressure the reservoirs. Locking shaft collars secure the dye injection assembly at the desired height. When full, the water level of the HSWT in a closed-channel configuration is higher than the gravity-fed dye system can be realistically operated. Therefore, it is used only in an open-channel configuration. Custom blocks mount the assembly to the rail system (see Fig.4.12). The bottom platform incorporates needle valves at the drain point of each reservoir for fine flow control. The

needle valves mate with 3/16" I.D. flexible tubing. As with the acrylic windows for the test section, cast acrylic is preferred for construction of dye systems.

4.3.3 Design: Pressurized Dye Injection

Unlike gravity-fed systems, pressurized dye injection systems can deliver dye whether they are placed above or below the waterline of the tunnel. For the HSWT, this allows dye to be injected in a closed channel configuration with the tunnel completely filled. In addition, pressurized systems deliver consistent flowrates and can achieve higher velocities.

To estimate how much pressure would be needed to achieve the desired flow rate of 3 m/s (9.84 ft/s), the Bernoulli equation was used [12]. Given that tubing and plastic pipe have a very low equivalent roughness and the tubing lengths are less than 1 m (3.28 ft), major head loss was assumed to be negligible for this estimation [12]. To model the worst case scenario, it was assumed that the test section was completely filled. Therefore, the pressure at the outlet nozzle was assumed to be equal to the hydrostatic pressure in the center of the test section with an exit velocity of 3 m/s (9.84 ft/s). The fluid velocity in the canister was set to zero, and the change in height was assumed to be negligible with the canister placed at the same elevation as the test section.

$$P_{canister} = P_{nozzle} + \gamma \left(\frac{V_{nozzle}^2}{2g} \right) \tag{4.3}$$

Equation 4.3 estimates that a canister pressurized to approximately 62 kPa (9 psi) will supply the dye from the nozzle tip at 3 m/s (9.84 ft/s) with the HSWT in a closed-channel configuration.

The canister chosen is a standard 254 mm (10") clear polypropylene water filter housing, with a maximum rated pressure of 689.5 kPa (100 psi). Though the high pressure rating is not necessary to achieve the desired flow rate, it is a precaution against accidental connection

of the canister to an improperly regulated air source. The concept of operation for the dye canister is illustrated in Fig. 4.13a and the assembled unit is shown in Fig. 4.13b. The canister has 1/4" NPT inlet and outlet ports that are adapted with pneumatic fittings to connect standard 1/4" O.D. air tubing. Teflon tape is for threaded adapters throughout the assembly to promote a water tight seal.To provide a path for the dye to flow out of the filter housing, a 19 mm (3/4" O.D.) ABS plastic tube is cut to reach the bottom of the canister and epoxied into the outlet passage of the filter housing cap using a plastic-safe epoxy.

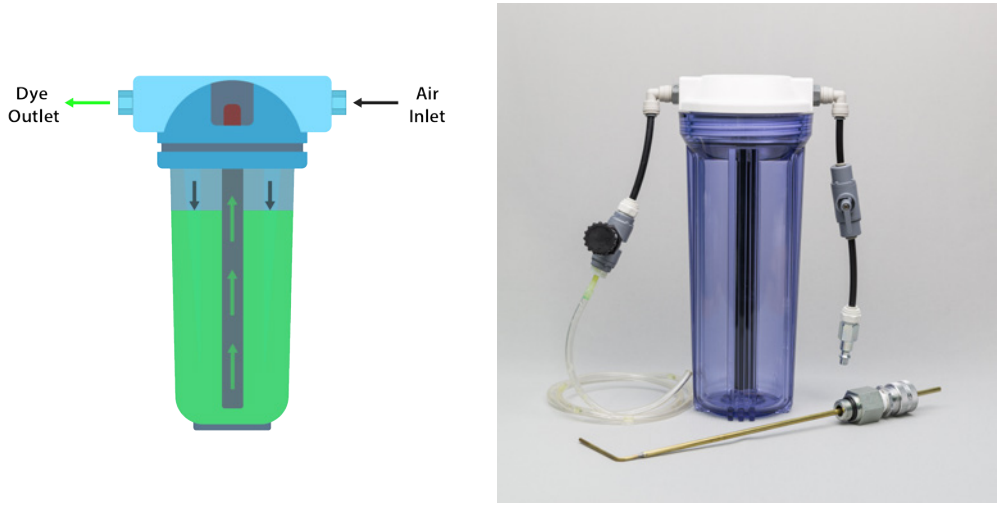

(a) (b)

Figure 4.13: (a) Illustration of pressurized dye concept of operation (b) Assembled pressurized dye system with an injection nozzle

On the inlet side of the canister, 1/4" O.D. tubing is connected to another 1/4" NPT to 1/4" O.D. tube adapter combined with a standard male quick-connect adapter for air compressor hoses. A precision control needle valve connected to the outlet of the canister is outfitted with a 1/4" NPT to 1/4" tube adapter on the valve inlet and a 1/4" NPT to 3/16" ID barb on the valve outlet. The flexible tubing connects the dye canister to the injection nozzles discussed in the following section.

4.3.4 Design: Nozzles and Mounts

Brass hobby tubing and stainless steel tubing are used to construct dye injection nozzles for the HSWT. Despite the lack of corrosion resistance for long term use, the brass hobby tubing offers a number of advantages in building injection nozzles. The sizes of brass hobby tubing are designed to fit within one another, allowing for telescoping of tubing sizes. In addition, the tubing can be easily be soldered together without the need for a specialty solder as is the case with stainless steel tubing, which requires silver solder. The nozzle tubing at the attachment point is 3/16" O.D., where 3/16" I.D. flexible tubing is used to connect nozzles to the dye reservoirs. A similar calculation to that done for the pneumatic hammer in Section 3.3 was performed to size nozzle tubing that will withstand fluid drag forces up to 3 m/s (9.84 ft/s). However, the moment of inertia was calculated for a hollow tube as shown in Equation 4.4 below.

$$I_o = \frac{\pi}{4}\left(r_o^4 - r_i^4\right) \tag{4.4}$$

Nozzles are used conjunction with the traverse discussed in Section 3.4. A 305 mm (12") long angle bracket was modified to accommodate a sliding block drilled to accept and secure injection nozzles as shown in Figure 4.14. In this configuration, dye injection nozzles can be traversed the entire length, width, and height of the test section.

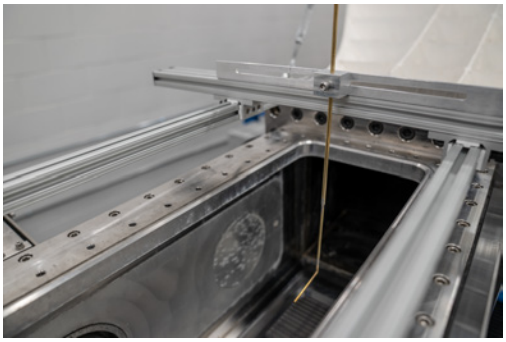

Figure 4.14: Injection nozzle clamp attached to the test section traverse

4.3.5 Selection: Dye

Based on existing literature and first hand experimentation it was found that red, blue, and green dyes generally produce the clearest contrast as compared to other colors, particularly when combined with a white background. Gel-based dyes perform poorly as compared to liquid dyes, as gels are slow to mix and clog needle valves. The HSWT has a water volume of approximately 10.6 m^3 (2,800 gal) and traditional food coloring dyes did not significantly pollute the water column for experiments requiring 4-6 reservoirs of dye from the gravity-fed system, or 1 canister from the pressurized system. Maintaining proper chlorine levels and filtration greatly influences the dissipation of dyes as discussed in Section 5.1.

Biodegradable fluorescent dyes are also used in the HSWT. These fluorescent dyes are commercially sold as "tracing" or "leak detection" dyes. When the fluorescent dye is combined with an ultraviolet light, it provides an insightful and visually stunning display that photographs with rich contrast and detail (see Fig. 4.15).

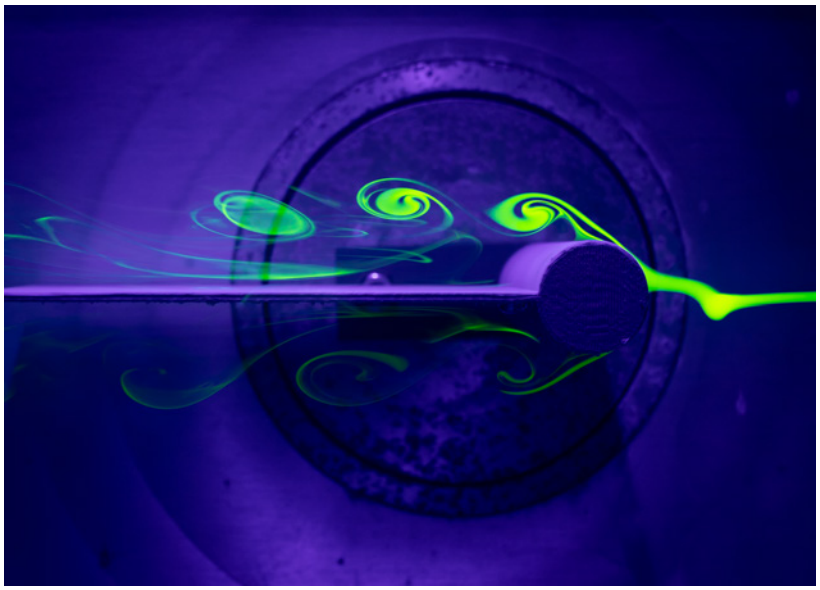

Figure 4.15: Vortex formation over a splitter plate shown with fluorescent dye

Fluorescent dyes are potent when combined with an ultraviolet light and can be mixed 1:200 parts dye to water, making them cost effective. The disadvantage of fluorescent dyes

is that fewer colors are readily available than food dyes and therefore are less suited to experiments requiring the use of more than two colors simultaneously. Another advantage of the potency is that the specific gravity of the dye mixture remains very close to that of the water itself and does not require readjustment. The specific gravity of dye mixtures not well matched to water causes the dye streamlines to drift even in uniform flow. Mixtures that display an appreciable drift should be adjusted for accurate flow visualization. For example, ethyl alcohol can be used to offset mixtures that are too heavy.

In both gravity-fed and pressurized systems, the dye exit velocity must be equal to the local flow velocity to accurately model streamlines. The correct exit velocity is indicated when the dye appears as a smooth filament (Fig. 4.16a). Turbulent wake structures will form when the exit velocity is too high (Fig. 4.16b), and a thin filament will be formed when the exit velocity is too low (Fig. 4.16c).

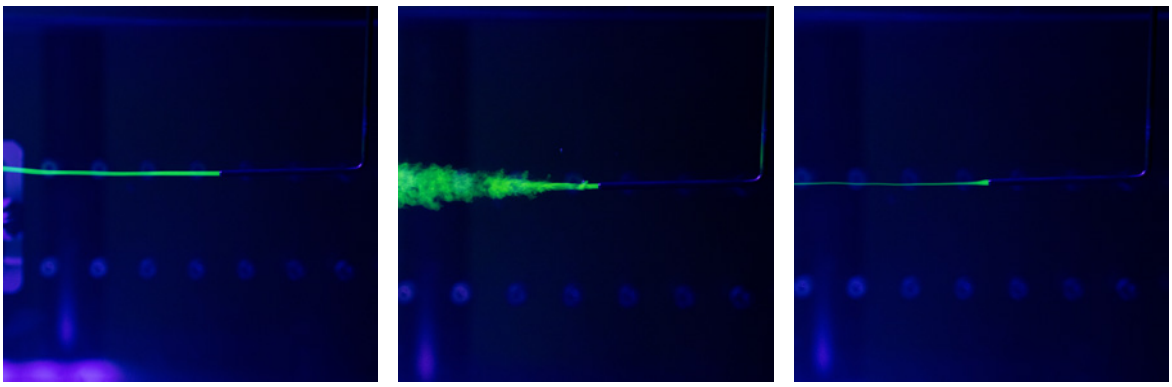

(a) (b) (c)

Figure 4.16: (a) Correctly formed dye filament. (b) Broken dye filament indicating excessive dye flowrate (c) Thin line filament indicating insufficient dye flowrate

4.3.6 Results and Discussion

While the pressurized dye injection system is properly designed to inject dye up to speeds of 3 m/s (9.84 ft/s), flow visualization is most effective at speeds below 0.5 m/s (1.64 ft/s). The primary reason that flow visualization fails to work at higher speeds is that the dye dissipated too quickly to observe the flow around a test article. While high-speed cameras can be used to observe dye flows at higher speeds, they are expensive and require proper lighting to function properly. In addition, the wake pattern of the dye injection nozzle becomes more disruptive to the flow at speeds above 0.5 m/s (1.64 ft/s), causing turbulence in the dye streamline. This is attributed to the density of water causing the Reynolds number of the nozzle to quickly enter transitional and turbulent flow regimes. Fairings can be added to the injection nozzles to smooth the flow around them. However, the size of the fairing needed to achieve smooth flow quickly becomes unrealistically large as speed increases. Placing the nozzle far upstream of the test article will maximize the recovery of vortices shed by the nozzle. If the dye filament separates before reaching the test article, it should be moved downstream until the filament is able to reach the model in a smooth streamline (see Fig. 4.16a).

Despite these challenges, the pressurized dye injection system remains an asset to HSWT operators. The chief advantage of this system is that it can be placed away from the test section and at a large range of elevations. Compared to low-speed water tunnels, the test sections of high-speed water tunnels are relatively small. Performing experiments with the gravity-fed dye injection system suspended above a small test section can quickly become cumbersome depending on the experiment being conducted.

Chapter 5

Maintenance

To keep the HSWT operational, the structure and water quality of the tunnel must be preserved and a number of machine components must be serviced and replaced throughout the lifetime of the water tunnel. The first two sections of this chapter discuss techniques for water quality and corrosion management. The remaining sections cover the service of machine components. This chapter will familiarize operators with the responsibilities involved with maintaining the tunnel, which includes first-hand preventative maintenance and scheduling service with the UGA Instrument Shop. While many components are replaced and serviced on an as-needed basis, Table 5.1 provides a summary of scheduled maintenance tasks. An extensive list of commonly replaced components is provided in the appendix.

Service Description	**Interval**
Chlorine Dosing (50 ml)	Weekly
Propeller Anode Replacement	Biannual or when 50% depleated
Water Replacement	Annual
Bearing Relubrication	Annual
Nitrile Bellow Replacement	6 years

Table 5.1: Summary of scheduled maintenance tasks

5.1 Water Management

Maintaining water quality in a water tunnel promotes optical clarity, protects instrumentation from damage, and prevents organic matter from growing in the tunnel. A water management system (WMS) was constructed for the HSWT using commercially available materials. The major components of the water management system in include a pump, filter, and storage tank. The WMS serves to maintain the water quality in the tunnel and to drain or fill the tunnel for experiments and maintenance. The selection and setup of each component will be detailed in this section. An illustration of the WMS is provided in Figure 5.1 to accompany the description of each component.

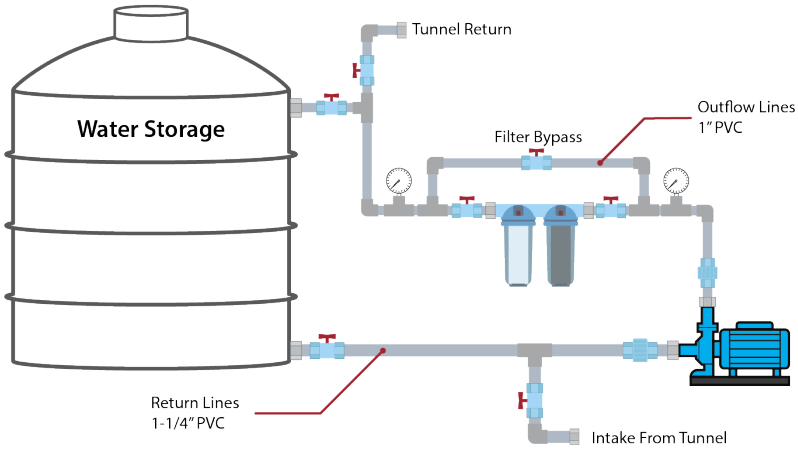

Figure 5.1: Illustration of the water management system

The pump and filter system are sized according to criteria commonly used for swimming pools, which require that the total water volume be circulated three times in a 24-hour period.[19]. With approximately 10.6 m^3 (2,800 gal) of water volume, the minimum desired flow rate for the filter is approximately 22 L/min (5.8 gal/min). A 746 W (1 HP) motor (Fig. 5.2a) was selected with a flow rate capacity up to 20 GPM (4.6 m^3/hr) and head pressures up to 57 m (82 psi, 190 ft) [20]. The pump is intentionally oversized, as the pump

also serves to transport water from the storage tank back to the tunnel. Exchanging test articles and test section windows requires that approximately 3 m^3 (800 gallons) be removed from the HSWT to lower the water level below the test section. Therefore, a high flow rate is desired to minimize down time between experiments. For filtering, the pump is operated continuously for many hours at a time. Oversizing the pump reduces the risk of overheating during filtration by operating well below the maximum flow rate of the pump. The pump is placed below the tunnel to minimize pump cavitation at high flow rates, using the hydrostatic pressure to provide Net Positive Suction Head (NPSH).

(a) (b)

Figure 5.2: (a) Filter pump and manifold (b) Filtration unit

Filtration for the HSWT comprises both mechanical and chemical filtration. Mechanical filtration is provided in the form of sediment filter cartridges that remove dirt, construction debris, rust and many other substances that degrade water quality. Two clear single cartridge filter housings (Fig.5.2b) rated up to 68 L/min (18 GPM) are used for filtration. Placing two filter housings in series prolongs the life of the filter cartridges by placing a course filter upstream from a finer filter to prevent the finer filter from becoming prematurely clogged with oversized debris. For general sediment removal, pleated cartridges rated to 20μm come standard with most single-cartridge filter housings and have been effective for general filtration of the HSWT. Finer filters reduce the flow rate of the filter system and

are used to remove specific debris, such as seeding particles. This applies to activated carbon filter cartridges as well, which can be exchanged with the downstream sediment filter to chemically purify and clarify the water [21]. The upstream filter housing of the HSWT typically remains without a filter cartridge to collect large debris, such as silicone from tunnel construction, that sink to the bottom of the filter bowl before reaching the filter cartridge located in the downstream housing. Shutoff valves are located on either side of filters to limit spillage during filter cartridge replacement.

Chemical filtration addresses contaminates such as sulfur, volatile organic chemicals, and bacteria. Household bleach is used to chlorinate the HSWT as a form of chemical filtration. Chlorine prevents organic growth in the water column and is effective in neutralizing dye from flow visualization experiments. A concentration of 0.3-0.5 parts per million (ppm) is sufficient to stunt organic growth and provide adequate water clarity [22]. Many water tunnels can temporarily withstand a shock treatment with higher concentrations of chlorine to resolve many common issues including the removal of chloramine bonds, killing algae, and pathogens. The level of chlorine concentration required for a shock treatment is case specific and should take into account parameters such as the construction material of the tunnel. If a water tunnel is constructed of metal, elevated levels of chlorine can accelerate corrosion. Acceptable chlorine concentrations depend on the type of metal. Shock treatments are used to accelerate the neutralization of dyes. The concentration required to neutralize dyes depends on the type of dye used, level of pollution, and desired rate of neutralization. At a chlorine concentration of 1 ppm, the biodegradable fluorescent dye used in the HSWT neutralizes in under an hour if polluted with one canister of dye mixed 1:200 dye to water. The use of live animals for testing should be avoided in water tunnels not specifically designed for such activities, which includes water tunnels that use chlorine for sanitation. Chlorine levels should be regularly monitored through the use of pool or aquarium test kits. To dose chlorine using a bleach solution, Equation 5.1 can be used as follows:

$$\gamma = \frac{(\sigma_c - \sigma_d)V}{\epsilon} \tag{5.1}$$

where γ is the volume of chlorine solution required in m^3, σ_c is the current chlorine concentration in ppm, σ_d is the desired chlorine concentration in ppm, V is the volume of water in m^3, and ϵ is the percent sodium hypochlorite in the chlorine solution multiplied by 1,000,000. For example, if the chlorine concentration must be raised from 0.1 ppm to 0.3 ppm for 10.6 m^3 (2,800 gal) of water volume, a common household bleach solution with a 12.5% sodium hypochlorite concentration will require 16.96 mL of bleach solution. As a baseline, water testing and chlorine dosing is performed on a weekly basis. Additional dosing is provided on an as needed basis when dyes or other contaminates are introduced into the water column.

The WMS is a closed loop, meaning that no water is drained from the system unless necessary for maintenance. A 11.35 m^3 (3,000 gal) storage tank was procured to retain the total water volume within the HSWT. The additional water volume is used to provide head pressure to the pump during filling as the tank nears empty. When filling the HSWT from the tap, the water is passed through the filter to prevent contaminates from entering the WMS. While standard PVC pipes and fittings are used for the WMS, high quality union ball valves are used throughout the entire assembly. Unlike less expensive valves, these valves remain easy to turn throughout their lifetime and can be disassembled for service. Failing to place unions and quality valves in the pipe network can have costly repercussions, which often involves the replacement of the entire plumbing network. As shown in Figure 5.1, unions are placed on each side of the pump for easy disassembly in the event that foreign particles become lodged in the pump. The pressure gauges located on either side of the filter assembly aid in monitoring filter cartridge status, as the pressure drop across the filters will increase as the cartridges are depleted. For expedited filling during experimentation, a filter bypass is incorporated into the pipe network. Any time the tunnel is not in operation, the

plumbing network is configured to recirculate and filter the water in the tunnel. For longer periods of inactivity, the water in the storage tank is exchanged with chlorinated water from the tunnel weekly to prevent the growth of bacteria. The tunnel is drained completely each year to eliminate the buildup of contaminates that otherwise cannot be effectively removed with filtration.

5.2 Galvanic Corrosion

5.2.1 Overview

High-speed water tunnels are commonly constructed from stainless steel. Dissimilar metals are typically present in the tunnel such as the pump propeller, honeycomb, test articles, or instrumentation. When dissimilar metals are placed in an electrolyte solution, such as saltwater or freshwater with impurities, one metal will serve as an anode and the other a cathode, causing a current to flow between them. To feed current, metal ions are stripped from the anode so that electrons can be exchanged with the cathode. This process, commonly known as galvanic corrosion, causes the anode to physically deteriorate. The closer the dissimilar metals are to each other, the faster the corrosion will occur. Galvanic corrosion can cause major damage to a water tunnel if not monitored and controlled. The galvanic series determines the nobility of metals and semi-metals, and reference charts readily available to determine the nobility of metals. Fortunately, there are simple and relatively inexpensive ways to combat galvanic corrosion, which include the use of sacrificial anodes and anodization.

5.2.2 Sacrificial Anodes

Stainless steel is high on the nobility chart as compared to metals such as aluminum or brass commonly used for test articles and test fixtures. If the water tunnel is constructed out of a metal such as stainless steel, placing a metal of higher nobility, such as silver, gold, or titanium, is discouraged as it will cause deterioration of the tunnel. Therefore, objects placed within the tunnel should be of lower nobility or made of a non-metallic material. Sacrificial anodes are low nobility metals that can be used to protect test articles, test fixtures, and components of the tunnel made of dissimilar metals. Sacrificial anodes are commercially available in a variety of shapes and sizes, often designed to protect boat components. The bronze propeller of the HSWT has been outfitted with a specialized propeller nut designed to host a sacrificial anode (Fig. 5.3). The propeller, prop nut, and sacrificial anodes for the HSWT are commercially sourced.

(a) (b)

Figure 5.3: (a) A newly installed anode on the propeller. (b) An anode aged 6 months and in need of replacement.

Aluminum and magnesium anodes are the best choice for freshwater applications, as zinc will quickly crust over and become ineffective in freshwater. Magnesium is the most quickly consumed of the sacrificial metals, but it is one of few options that will readily work in freshwater when attempting to protect aluminum from corrosion. The sacrificial anode must be in clean metal to metal contact with the material it is protecting in order to work properly. Guidelines from the boating industry suggest that anodes should cover 1-2% of the surface area being protected, and anodes should be replaced when they are 50% depleted. [23] This can be carried out on the HSWT by draining the water below the shaft, and accessing the anode through the viewport located downstream of the propeller.

5.2.3 Anodization

In addition to sacrificial anodes, anodization can be used to protect water tunnels and the objects within them. Anodizing is an electrochemical process that converts the metal surface into a durable, corrosion-resistant, anodic oxide finish. Aluminum is the most commonly anodized metal, although other nonferrous metals, such as magnesium and titanium can also be anodized [24]. Anodization is an effective and inexpensive method to combat corrosion under circumstances where sacrificial anodes may be impractical. As mentioned previously, a colored anodization coating visually reflects the condition of the coating more clearly than a clear anodization coating.

5.3 Machine Components

Each machine component of the HSWT requires manufacturer-specific installation, service, replacement, and troubleshooting procedures that are often available through the manufacturer's website. This section will cover the general information needed to monitor the status of machine components and schedule service when necessary.

5.3.1 Test Section Threading

The test section of the HSWT are exchanged multiple times a week for experimentation. Therefore, it is critical to protect and preserve the threaded holes used secure the windows to the test section (Fig 5.4a). The threaded holes of the test section frame must stay intact for the HSWT to reach its 25+ year service life. Stripping of the internal threads is difficult if not impossible to repair, and should be prevented at all costs. The primary preventative measure against stripping and screw breakage is an anti-seize compound lightly coated on the tips of the cap screws. Screws must be secured gently to prevent stripping. Though a broken screw can be removed, the process is time consuming and costly.

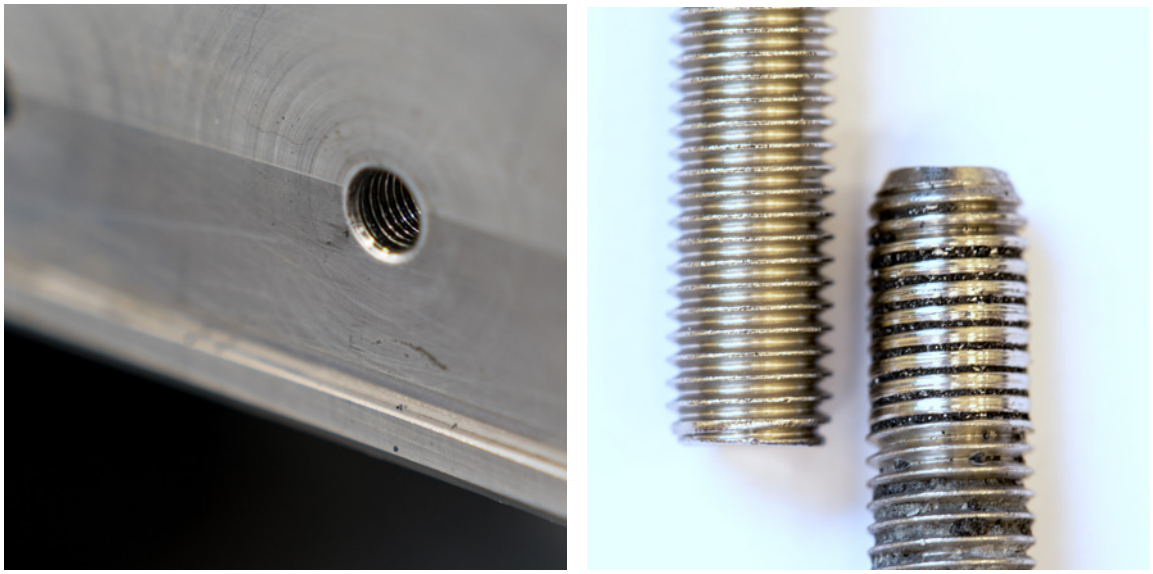

(a) (b)

Figure 5.4: (a) Threaded hole of the test section frame (b) Comparison of new screw (left) and badly stripped screw (right) that should be discarded

Whether a cordless drill or allen wrench is used to tighten the cap screws, the threads should first be engaged by hand. Screws that fail to engage with finger tightening should be inspected for fouling and stripping. Fouled screws can be cleaned with a clean rag or paper towel. Heavily fouled screws should be soaked in a solvent such as acetone and scrubbed

clean with a wire brush. Anti-seize should be reapplied after cleaning. Stripped screws (see Fig.5.4b) should be disposed of immediately and replaced. Should screws in good condition fail to engage with the internal threads, a screw can be omitted from that location until the hole can be cleaned or rethreaded. Several screws can be missing from the window without affecting its ability to seal properly.

Screws that resist fully seating should never be forced into the test section. If a cordless drill is used, the drive speed should be slow, and the clutch on the drill should be engaged to protect against over tightening. The UGA Instrument Shop should be contacted to clean and rethread holes as needed. However, holes can only be rethreaded a few times before the threading material has been stripped away, rendering the hole unusable. With proper care and regular cleaning, the service life of the test section frame will be extended.

5.3.2 Gaskets

Upon installation, the HSWT was equipped with o-rings to seal the test section windows. However, the o-rings were increasingly difficult to seat properly after multiple window exchanges. The o-rings have subsequently been replaced with custom gaskets fabricated from 3.175 mm (1/8") rubber reinforced with nylon fabric (see Fig. 5.5).

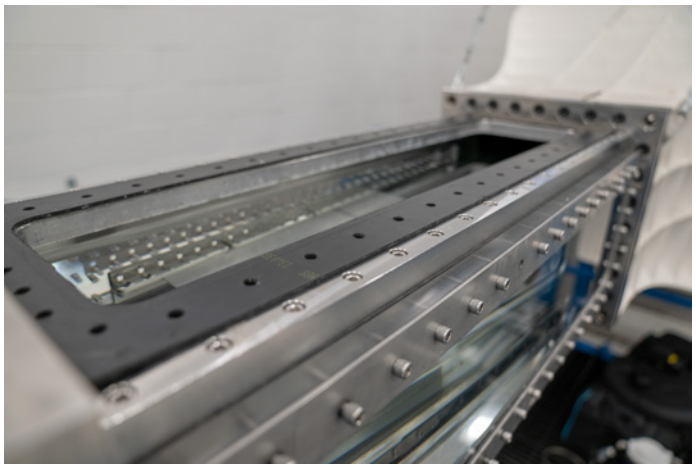

Figure 5.5: A gasket positioned on the top of the test section frame

The reinforced rubber provides and effective seal while not excessively deforming under compressive loads, and is used throughout the HSWT. The gaskets have oversized thru holes for the windows screws to prevent the gasket material from fouling the screws.

5.3.3 Belts

V-Belts are used to transfer the rotary motion of the motor to the propeller shaft of the HSWT (see Fig. 5.6). The belts are inspected for signs of wear each time the tunnel is operated. Improperly tensioned belts are the most common cause of belt slippage, squealing, heat build-up, and wear. If the belts begin to slip, make excessive noise, or flap uncontrollably it is a sign that the belts are improperly tensioned. Tensioning procedures should be followed as detailed by the belt manufacturer [25].

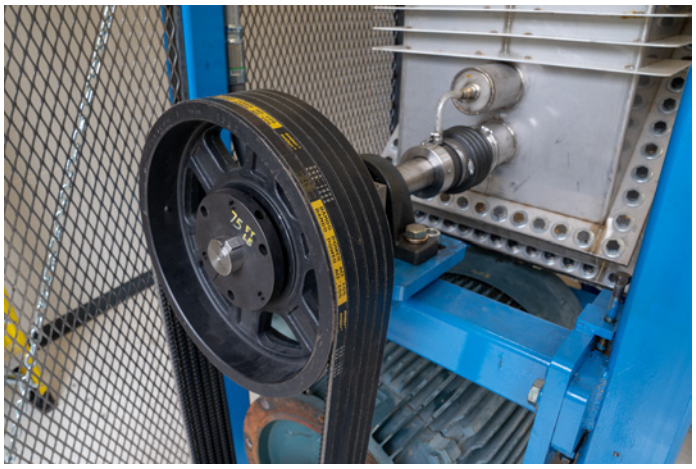

Figure 5.6: Motor belts of the HSWT after one year of use

Belt life is dependent operating climate, tension, and speed, and is therefore difficult to accurately predict. Visual indicators that warrant belt replacement include fraying, cracking, and erosion of the belt material. Belts will need to be re-tensioned periodically as they age; however, severe slippage at low to medium motor speeds is an indication that the belts need replacement. Service of the belt system is performed by the UGA Instrument Shop. The motor should be stopped and locked out any time the belts are being serviced.

5.3.4 Bearings

Three types of bearings are installed on the HSWT including a pillow block bearing, a thrust bearing (Fig. 5.7a) and a cutless bearing (Fig. 5.7b). The pillow block bearing and cutless bearing support the weight of the propeller shaft while thrust bearing counteracts the thrust created by the rotation of the propeller. Proper lubrication of the bearings will reduce the friction in the bearing, reduce wear, and prevent corrosion. Both the pillow block and thrust bearing incorporate a grease port that allows the bearing to be relubricated. The lubrication interval depends on the bearing type, operating temperature, humidity level, and cleanliness of the environment in which the bearing is being operated. The HSWT is located in a clean indoor environment. Annual lubrication should be used as a guideline [26].

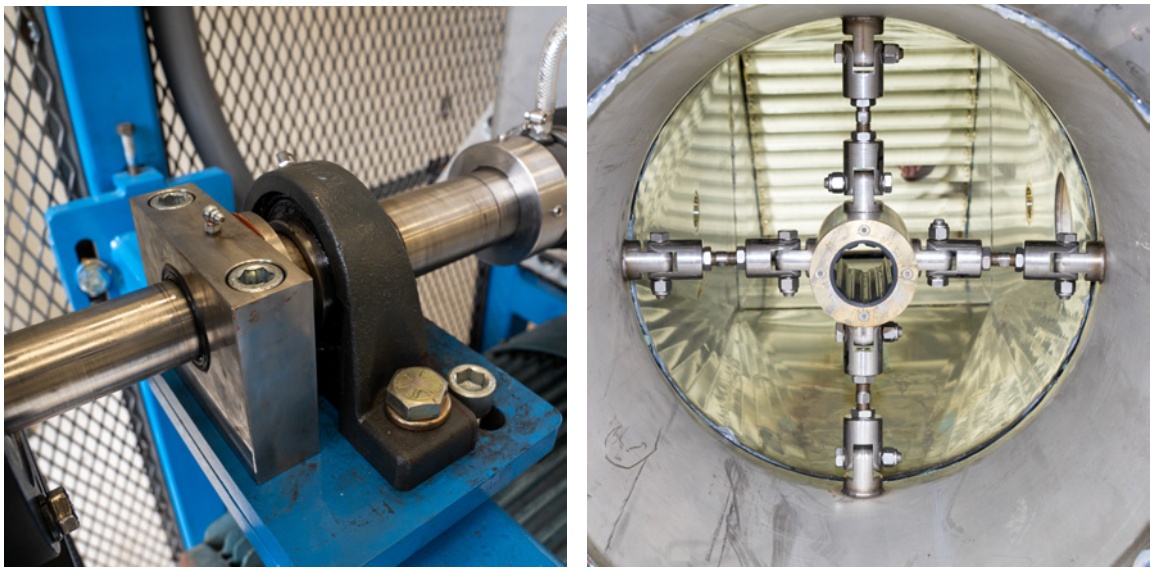

(a) (b)

Figure 5.7: (a) Pillow block and thrust bearing (b) Cutless bearing inside the propeller housing

Bearing service and replacement should be carried out by the UGA Instrument Shop. Unlike pillow block and thrust bearings, cutless bearings are specially designed to operate while fully submerged in water, using a fluted rubber tube to create a hydrodynamic film

for lubrication. These bearings can have a ten year life expectancy, but this figure will vary with use, shaft alignment and environmental conditions [27]. Vibration and squeaking are indicators that bearings are in need of service or replacement.

5.3.5 Shaft Seal

The HSWT is equipped with a packless shaft seal that creates a water-tight penetration point for the propeller shaft (see Fig.5.8). A packless shaft seal, also known as a carbon-faced seal, is a mechanical seal created between a rotating collar and a stationary carbon flange.

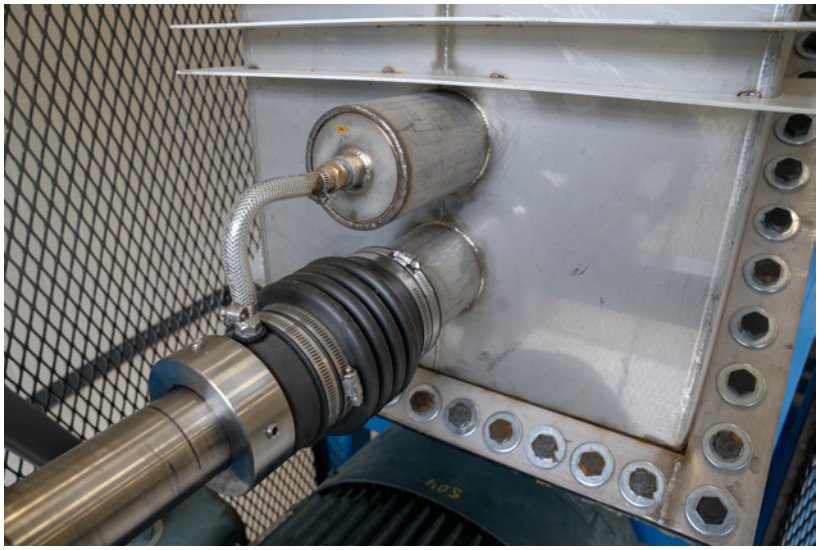

Figure 5.8: Packless shaft seal installed on the HSWT

Packless seals require a higher up-front cost than packing seals but they seldom need replacement under normal operating conditions and have a specially designed passage for water to cool and lubricate the seal faces with little to no leakage [28]. The nitrile bellow of the shaft seal should be replaced every six years, per the manufacturer's recommendations [29]. Vibration, squeaking, and leaks are indications that service is needed outside of preventative maintenance. Bellow replacement and service of the shaft seal should be carried out by the UGA Instrument Shop.

Chapter 6

Conclusion

While water tunnels are predominately used to study hydrodynamics and cavitation, the HSWT will primarily serve to progress the field of fluid-structure interaction. This class of problems includes coupled phenomena between a structure and a surrounding fluid that would otherwise not occur if the structure and fluid are considered separately. The potential of the HSWT has begun to emerge in the first year of operation, having yielded novel findings in the areas of underwater flutter, vortex-energy capture, and hydroelastic damping. The principles, devices, and procedures summarized in this thesis provide the foundation necessary for progressive experimentation in the HSWT throughout its service life. More information about the water tunnel (including calculations, part numbers, and drawings) is available by request from the author via e-mail.

6.1 Forward Work

A brief list of suggested equipment and improvements for the Dynamic Devices and Solutions Lab are provided below:

Desired Instrumentation

- Particle Image Velocimeter
- Digital Image Correlation System
- Sting-Mount 6-Axis Force Balance

Desired Improvements

- Sound proofing or replacement of motor to minimize disturbance of lab members while operating the HSWT
- Additional signal conditioner for force balance
- Additional UV light and fluorescent dye color for flow visualization
- Construction of hydrogen wire system for flow visualization
- Full characterization of electromagnetic interference in force balance measurements
- Complete automation of filling and draining process using an industrial controller
- Ribbing of round to square transition for increased operating pressure
- Installation of access port above propeller for ease of service and repair
- Replacement of burst disc with 5 psi vacuum sensitive disk
- Flow-loop comparison of computational estimates to experimental estimates
- Large air compressor to improve pneumatic hammer and pressurized dye consistency

Bibliography

[1] F. P. Beer, J. E. Russel Johnston, J. T. DeWolf, and D. F. Mazurek, *Mechanics of Materials*. McGraw HIll, 2012.

[2] I. Nedyalkov, "Design of contraction, test section, and diffuser of a high-speed water tunnel," Master's thesis, Chalmers University of Technology, 2012.

[3] R. Etter and M. Wilson, "The large cavitation channel," in *Proc. 23rd American Towing Tank Converence (New Orleans, LA)*, 1992.

[4] Engineering Laboratory Design Inc., *Texas Christian University 45cm Flow Visulization Water Tunnel Specifications*, Sept. 2014.

[5] Engineering Laboratory Design Inc., *Bettis Atomic Power Laboratory - 30 fps Water Tunnel Specifications*, Sept. 2011.

[6] M. Oyeyemi, "Design and qualificaiton of the uga water tunnel," Master's thesis, University of Georgia, 2017.

[7] *Occupational Noise Exposure*, no. CFR 29 Part 1910.95, Occupational Safety and Health Administration, 2018.

[8] L. Daniel, S. Mohagheghian, D. Dunlap, E. Ruhlmann, and B. R. Elbin, "Design of a recirculating water tunnel for the study of high-reynolds number turbulent boundary

layers," in *ASME 2015 International Mechanical Engineering Congress and Exposition*, ASME, 2015.

[9] E. A. Rasquin, S. Lynn, and D. N. Hanson, "Vacuum degassing of carbon dioxide and oxygen from water in packed columns," tech. rep., Department of Chemical Engineering, University of California Berkeley, 1977.

[10] S. Roth, M. Calmon, M. Farhat, C. Muench, M. Huebner, and F. Avellan, "Hydrodynamic damping identification from an impulse response of a vibrating blade," in *3rd IAHR International Meeting of the Workgroup on Cavitation and Dynamic Problems in Hydraulic Machinery and Systems*, 2009.

[11] M. Farhat and F. Avellan, "Dynamic calibration of transient sensors by spark generated cavity," in *Proceeding of IUTAM Symposium on Bubble Dynamics and Interface Phenomena*, 1993.

[12] B. R. Munson, T. H. Okiishi, W. W. Huebsch, and A. P. Rothmayer, *Fundamentals of Fluid Mechanics*. John Wiley & Sons, Inc., 7th ed., 2013.

[13] E. Kohtanen, "Hydroelastic damping of low aspect ratio plates," in *71st Annual meeting of the APS Division of Fluid Dynamics*, 2018.

[14] Validyne Engineering, 8826 Wilbur Ave. Northridge, CA 91324, *P55 Pressure Transducer Handbook*, 2018.

[15] Dantec Dynamics, 16-18 Tonsbakken, DK-2740 Skovlunde, Denmark, *Flow Exporer Laser Doppler Anemometer*, 6th ed.

[16] R. Therrien, S. Roux, B. Comtois, and M. Wosnik, "Design of a high speed water tunnel force balance & testing of high performance hydrofoils for marine hydrokinetic turbines," tech. rep., University of New Hampshire, 2012.

[17] National Instruments Inc., *Strain Gauge Measurement - A Tutorial*, 08 1998.

[18] Vishay Precision Group, *Noise Control in Strain Gauge Measurements*, tn-501-2 ed., 07 2013.

[19] INYO Pools, *How to Size a Pool Filter*.

[20] Xylem Inc., 2881 East Bayard St. Seneca Falls, NY 13148, *Goulds LB Booster Pump Technical Brochure*, 2016.

[21] Keystone Filtration, *What is Carbon Filtration?*

[22] A. J. Smits and T. Lim, *Flow Visualization: Techniques and Examples*. IMPERIAL COLLEGE PR, second ed., Sept. 2012.

[23] SeashieldMarine, "What are zincs on a boat?." Web Article, Nov. 2014.

[24] Aluminum Anodizers Council, *What is anodizing?*, 2017.

[25] Bando, *V-Belt and Timing Belt Installation and Maintenance*.

[26] KML Bearing USA, *KML Bearing Training Manual*.

[27] Duramax Marine, *Duramax Marine Installation and Storage Manual for Flanged Cutless Bearings*, 2018.

[28] PYI Inc., *PSS Shaft Seal Catalog*.

[29] PYI Inc., *PSS Shaft Seal Installation Instructions*.

Chapter 7

Appendix

Frequent Replacement Items

Component	Manufacturer/Source	Part Number	Additional Details
Cap Screws (Acrylic Windows)	McMaster-Carr	92185A614	5/16-24 x 1 1/2" (316 Stainless)
Cap Screws (Metal Windows)	McMaster-Carr	92185A617	5/16-24 x 1" (316 Stainless)
Filter	McMaster-Carr	7191K13	20" Pleated Filter - 20 micron
Replacement Propeller Anode	BoatZincs	Model H	2" Shaft Size, Magnesium
Chlorine Test Reagent	Bulk Reef Supply	208236	Total Chlorine Reagent for HI711
Rail Fasteners	McMaster-Carr	47065T226	Drop-in Fastener with Ball, 1/4"-20 Thread for T-Slotted Framing
Fluorescent Dye	EcoClean/Amazon	52146, 52146	Green, Red
Force Balance Plug Face O-Ring	McMaster-Carr	9452K518	Dash # 362
Force Balance Plug Radial O-Ring	McMaster-Carr	9452K412	Dash # 354
Force Balance Key Slot O-Ring	McMaster-Carr	9452K17	Dash # 017
Force Balance Rod Radial O-Ring	McMaster-Carr	9452K76	Dash # 022

Table 1: Reference table for frequently replaced parts

Infrequent Replacement Items

Component	Manufacturer/Source	Part Number	Additional Details
V-Belt	Bando Inc.	Power Ace Cog 5VX-1000	100" Effective Outside Length
Force Balance Flex Seal	McMaster-Carr	8633K54	1/8" Natural Latex Rubber, 40A Durometer
Shaft Seal	PYI Inc.	PSS 2-1/2" GE	4" Stern Tube
Cutless Bearing	Duramax Marine/Motion Industries	860642100	2 1/2" Shaft Diameter
Thrust Bearing	KML	SKF 51210	
Pillow Block Bearing	KML	UCP213-40	
Propeller	Michigan Wheel.	364858	4 Blade Bronze 23x25 RH
Ball Valves	U.S. Plastics	20538, 20539	Part # for 1" and 1-1/4" valves
Filter Housings	Keystone Filtration/McMaster-Carr	9979T73	20" High Cartridge, Clear, 3/4 NPT, 20 gpm Flow
Prop Nut for Anode	BoatZincs	Model H	2" Shaft Size 1-1/2" NC 6 RH
Chord Grip (sized for dye nozzle)	McMaster-Carr	7529K305	Liquid-Tight Cord Grip, 1/2 Knockout Size
Chord Grip Adapter	Grainger	39A314	3/4"-16 x 1/2" NPT Conversion Adapter
Blacklight	OPPSK/Amazon	640007	9LED 19.7"x1.6"x1.6"
Dye Nozzle Tubing	K&S Engineering/Hobby Lobby	101329, 101196, 101154, 100503	3/16", 5/32" , 1/8", 3/32"
Dye Flexible Tubing	McMaster-Carr	5233K53	Slip-fit over 3/16" O.D. Tubing
Strain Gauge	Omega	SG-7/DY11	Dual strain gauges for force balance, 350 Ohm, matched for steel
Strain Gauge Glue	Omega	SG496	1 oz methyl-based cyanoacrylate (approx. 750 gages)
Strain Bridge Terminals Pads	Omega	BTP-4	
Shielded Cable	Magnetic Shield Corp.	MTH-24	Inter-8 Weave, Insulated and Shielded
Signal Conditioner	Omega	DMD4059	
Test Section Gasket Material	Kuriyama of America, Inc.	NCI-2P04x48x50	Chloroprene reinforced with nylon
Differential Pressure Transmitter	Validyne Engineering	P55D-1-N-1-42-S-3-A	Must specify desired diaphragm range
Riser Tank	Amtrol/SupplyHouse	ERTG-30	30 gallon retention tank
Pressurized Dye Canister	Bulk Reef Supply	200001	10" reverse osmosis canister, 1/4" Ports
Chlorine Test Kit	Bulk Reef Supply	208175	Hanna Checker - total chlorine colorimeter

Table 2: Reference table for infrequently replaced parts